Complete Structure of the Polysaccharide from *Streptococcus sanguis* J22†

Chitrananda Abeygunawardana‡ and C. Allen Bush*,‡
Department of Chemistry, Illinois Institute of Technology, Chicago, Illinois 60616
John O. Cisar
Laboratory of Microbial Ecology, National Institute of Dental Research, Bethesda, Maryland 20892
Received June 1, 1989; Revised Manuscript Received August 8, 1989

ABSTRACT: The cell wall polysaccharides of certain oral streptococci such as *Streptococcus sanguis* strains 34 and J22, although immunologically distinct, act as receptors for the fimbrial lectins of *Actinomyces viscosus* T14V. We report the complete covalent structure of the polysaccharide from *S. sanguis* J22 which is composed of a heptasaccharide subunit linked by phosphodiester bonds. The repeating subunit, which contains α-GalNAc, α-rhamnose, β-rhamnose, β-glucose, and β-galactose all in the pyranoside form and β-galactofuranose, is compared with the previously published structure of the polysaccharide from strain 34. The structure has been determined almost exclusively by high-resolution nuclear magnetic resonance methods. The ^1H and ^{13}C NMR spectra of the polysaccharides from both strains 34 and J22 have been completely assigned. The stereochemistry of pyranosides was assigned from J_{H-H} values determined from phase-sensitive COSY spectra, and acetamido sugars were assigned by correlation of the resonances of the amide ^1H with the sugar ring protons. The ^{13}C spectra were assigned by ^1H-detected multiple-quantum correlation (HMQC) spectra, and the assignments were confirmed by ^1H-detected multiple-bond correlation (HMBC) spectra. The positions of the glycosidic linkages were assigned by detection of three-bond ^1H–^{13}C correlation across the glycosidic linkage in the HMBC spectra. The positions of the phosphodiester linkages were determined by splittings observed in the ^{13}C resonances due to ^{31}P coupling and also by ^1H-detected ^{31}P correlation spectroscopy.

The cell wall polysaccharides of certain oral streptococci such as *Streptococcus sanguis* 34 are receptor molecules for the fimbrial lectin of *Actinomyces viscosus* (McIntire et al., 1988). These and other species coexist in large numbers on human teeth, and consequently, their lectin-mediated coaggregations probably contribute to microbial colonization (Cisar, 1986). The complete structure of the cell wall polysaccharide of *S. sanguis* 34 was determined by a combination of several methods which included selective chemical degradation, methylation analysis, mass spectrometry, and ^1H and ^{31}P NMR spectroscopy (McIntire et al., 1987, 1988; Abeygunawardana et al., 1989). Polysaccharide I is a linear polymer of a hexasaccharide repeating unit joined by phosphodiester bonds.

structure I

$$[\rightarrow PO_4^-\rightarrow 6)\text{-}\alpha\text{-D-}\underset{A}{Gal}p\text{NAc}(1\rightarrow 3)\text{-}\beta\text{-L-}\underset{B}{Rha}p(1\rightarrow 4)\text{-}\beta\text{-D-}\underset{C}{Glc}p(1\rightarrow 6)\text{-}\beta\text{-D-}\underset{D}{Gal}f(1\rightarrow 6)\text{-}\beta\text{-D-}\underset{E}{Gal}p\text{NAc}(1\rightarrow 3)\text{-}\underset{F}{\alpha\text{-D-}Gal}p(1\rightarrow]_n$$

The antigenic and lectin receptor activities of this polysaccharide must depend on distinct structural domains since the former involved α-linked *N*-acetylgalactosamine at the nonreducing end of the hexasaccharide unit while the latter appeared to depend on GalNAcβ(1→3)Gal at the reducing end (McIntire et al., 1988). Related observations with certain other steptococcal strains, such as *s. sanguis* J22, indicated that while the cell wall polysaccharides of these strains were antigenically distinct, they were all recognized by the lectins of *A. viscosus* and *Bauhinia purpurea* (Cisar et al., unpublished results). To establish the structural basis of these findings, further studies of the polysaccharides from different bacterial strains have been initiated. In this paper we report the determination of the complete covalent structure of the polysaccharide from *S. sanguis* J22 using high-resolution NMR methods including ^1H, ^{13}C, and ^{31}P NMR spectroscopy.

The utility of NMR spectroscopy in bacterial polysaccharide structure determination has been well established by published results from several different laboratories. ^1H NMR spectroscopy is often the method of choice for the otherwise difficult problem of the determination of the anomeric configuration of glycosidic linkages, especially of pyranosides. The nuclear Overhauser effect in ^1H NMR spectroscopy has also been used to provide information on carbohydrate sequence and intersaccharide linkage position. Unfortunately, since NOE depends on proton proximity rather than on bond connectivity, the presence of NOESY cross peaks depends on the conformation of the glycosidic linkage, and this experiment cannot provide a primary method for determination of the intersaccharide linkage for any new structure whose conformation is unknown. As a result of the dependence of NOE on glycosidic linkage conformation, the cross peak between the anomeric proton and the aglycon proton may be smaller than that between the anomeric proton and a proton adjacent to the aglycon proton. This situation, which has been observed in several complex oligosaccharides including the *S. sanguis* 34 oligosaccharide (McIntire et al., 1987), could lead to incorrect assignment of linkage if the NOE experiment is not supplemented with more primary linkage data such as methylation analysis.

^{13}C NMR spectroscopy has also been employed as an auxiliary method in a number of structure determination studies of bacterial polysaccharides, especially in the assignment of furanosides (Michon et al., 1988; Moreau et al., 1988). The recent introduction of ^1H-detected two-dimensional spectroscopy for correlation of the ^1H and ^{13}C spectra promises powerful new methods for simultaneous assignment of both

† Research supported by NSF Grant DMB-8517421.
‡ Present address: Department of Chemistry, University of Maryland Baltimore County, Baltimore, MD 21228.

0006-2960/90/0429-234$02.50/0

types of spectra, and it has recently been proposed that long-range $^{13}C-^{1}H$ correlation spectroscopy could be used as a primary method for determination of linkage in complex polysaccharide structures (Lerner & Bax, 1987; Byrd et al., 1987; Dabrowski et al., 1987). With proton-detected multiple-bond correlation ($^{1}H[^{13}C]$HMBC), these workers showed that it is possible to find three-bond coupling correlations across the glycosidic linkage. Since the correlation is transmitted through bonds, this method provides linkage information of a more fundamental type than that provided by the ^{1}H NOESY method, which gives information only on proton proximity. While the three-bond coupling constant across the glycosidic linkage does depend on conformation, only the size of the coupling constant and not its existence is in question. Therefore, $^{13}C-^{1}H$ correlation either between the anomeric carbon and the aglycon proton or between the anomeric proton and the aglycon carbon atom resonances provides unambiguous proof of glycosidic linkage position. Thus three-bond $^{13}C-^{1}H$ correlation can be used as the primary method for the rigorous proof of glycosidic linkage position. The method requires a complete and reliable assignment of both the ^{1}H and ^{13}C spectra for the interpretation of the HMBC data.

In this paper, we report the complete ^{1}H, ^{13}C, and ^{31}P assignments for the cell wall polysaccharide receptors of both *S. sanguis* 34 and *S. sanguis* J22. The NMR data on the *S. sanguis* 34 polysaccharide serve to validate the application of this new methodology for the structure determination of this type of complex polysaccharide, and the data on the polysaccharide from strain J22 represent the first determination of a new structure of this complexity completely by NMR spectroscopy. We argue that this method for NMR-based structure determination could have wide application in complex polysaccharide, glycolipid, and glycopeptide chemistry. The method is rapid and simple, lending itself to automation. Although the quantity of sample required falls in the range of 1–2 μmol, the method is not degradative, and the sample survives the procedure for use in studies of immunological properties and other biological activities or for further exploration of chemistry or three-dimensional conformation and interactions.

Materials and Methods

Isolation of Polysaccharides. Streptococcus sanguis strains 34 and J22 (Cisar et al., 1979) were cultured in 20-L batches of complex media and crude cell walls prepared as previously described (McIntire et al., 1988). Cell walls were suspended in 200 mL of 10 mM sodium phosphate buffer, pH 6.8, containing 10 mM $MgCl_2$ and 0.1% sodium azide and digested with 10000 units of mutanolysin (M-3765, Sigma Chemical Co., St. Louis, MO) for 1–2 days at 37 °C. Insoluble material was removed from the digest by centrifugation (15000*g*) and protein precipitated by the addition of trichloroacetic acid (TCA) to a final concentration of 5% (w/v). This step was performed in an ice bath. The TCA-soluble fraction was neutralized by the addition of tris(hydroxymethyl)aminomethane, dialyzed exhaustively against water containing a drop of chloroform, and lyophilized. This material was dissolved in 0.01 M sodium phosphate buffer, pH 8.0, applied to a (diethylaminoethyl)cellulose (DE52, Whatman, Inc., Clifton, NJ) anion exchange column, and eluted with a gradient of KCl (0–0.2 M) prepared in the starting buffer. Fractions were assayed for carbohydrate by the phenol–sulfuric acid method (Dubois et al., 1956) and for lectin receptor activity by an inhibition of hemagglutination assay using the lectin of *Bauhinia purpurea* (L-2501, E. Y. Labs, Inc., San Mateo, CA) and human O erythrocytes. Receptor polysaccharides were eluted from the anion exchange column in fractions containing 40–60 mM KCl and further purified by Sephacryl S-400 and S-300 (Pharmacia) gel filtration column chromatography. Each purified polysaccharide reacted as a single antigen in cross immunoelectrophoresis with antiserum prepared against whole bacteria of the corresponding strain. The isolation of these polysaccharides and their reactions with specific antibodies and lectins will be further documented in a subsequent paper (Cisar et al., unpublished results).

Sugar Composition and Absolute Stereochemistry. The carbohydrate composition of the polysaccharide samples was determined by HPLC of the perbenzoylated methyl glycosides according to the method of Jentoff (1985). Dried polysaccharide samples (100–200 μg) were methanolized by treatment with 0.2 mL of 1 M methanolic HCl at 80 °C for 4 h. The samples were dried under nitrogen and dissolved in 0.1 mL of dry methanol. A 50:50 mixture of pyridine and acetic anhydride (80 μL) was added to each sample and incubated at room temperature for 1 h to re-N-acetylate any hexosamines present. After mild methanolysis (0.1 M methanolic HCl, 65 °C, 30 min) each dried sample was redissolved in dry methanol and perbenzoylated by overnight incubation at room temperature in 0.1 mL of freshly prepared benzoic anhydride [5% benzoic anhydride and 10% (dimethylamino)pyridine in pyridine]. Reactions were stopped by addition of 0.9 mL of water, and each mixture was purified by extraction with 0.5 mL of toluene and by being washed three times with 1-mL portions of 5% $NaHCO_3$ and then with three 1-mL portions of 5% NaCl in 0.05 M HCl followed by three 1-mL portions of water. After the toluene was evaporated, the samles were dissolved in a 50:50 mixture of acetonitrile and water; 30 μL of each sample was injected into the HPLC. Reverse-phase HPLC analysis was carried out with a Waters automated HPLC equipped with a Kratos variable-wavelength UV/visible absorbance detector. A Spherisorb 3 μm C-18 ODS II (Alltech Associates) column (15 cm) was used.

The samples were eluted with a 50:50 acetonitrile/water mixture for 20 min followed by a single-step increase of acetonitrile to 60% for the rest of the run. The flow rate was maintained at 1.4 mL/min, and the column was equilibrated with a 50:50 solvent mixture for 20 min before each analysis. Eluents were detected by absorbance at 230 nm. Eluted fractions were collected and examined by circular dichroism. The peaks of the HPLC chromatograms were assigned from the retention times of perbenzoylated methyl glycoside samples prepared from the corresponding pyranosides.

The absolute stereochemistry of the sugar components was determined by vacuum ultraviolet circular dichroism spectroscopy in the 205–250-nm region on perbenzoylated monosaccharides collected from HPLC and on intact polysaccharides in the 170–230-nm region as described elsewhere (Kaluarachchi & Bush, 1989).

Nuclear Magnetic Resonance Spectroscopy. Spectra were recorded on a 500-MHz Bruker AM-500 spectrometer equipped with an Aspect 3000 computer or a 300-MHz Nicolet NT-300 spectrometer equipped with a 1280 computer and a 293C pulse programmer. The observed ^{1}H chemical shifts are reported relative to internal sodium 4,4-dimethyl-4-silapentane-1-sulfonate (DSS) with acetone as an internal standard (2.225 ppm downfield from DSS). The carbon chemical shifts are determined relative to internal acetone (31.07 ppm). The phosphorus chemical shifts are reported relative to the external reference signal of 85% H_3PO_4 contained in a sealed capillary tube.

Polysaccharide samples (10–20 mg) were exchanged three times in D_2O (99.8 atom % D) followed by lyophilization. The final solution was prepared by dissolving the sample in 350 μL of high-purity (99.96 atom % D) D_2O (Merck Sharp & Dohme Co.).

^1H spectra at 500 MHz were recorded with a spectral width of 2.6 kHz and 4K complex data points providing a digital resolution of 0.6 Hz/point. Resolution enhancement was achieved either by Gaussian transformation with line broadening of −2.0 and Gaussian broadening of 0.1 or by 10–15°-shifted sine bell transformation.

Two-dimensional ^1H–^1H correlation spectra at 300 MHz were obtained by the three-pulse sequence 90°–t_1–90°–90°–Acq, which (with proper phase cycling) allowed for coherence transfer through a double-quantum filter (DQF-COSY) (Rance et al., 1983). Two sets of 256 × 512 data points were acquired in adjacent blocks of memory, and the data were processed by the method of States et al. (1982) to obtain pure absorptive spectra. The total experimental time was 14 h. Prior to Fourier transformation, 30°- and 45°-shifted sine bell functions were used in the t_2 and t_1 dimension, respectively, and FID's were zero filled to obtain a final data matrix of 2K × 2K real points. The sweep width was 1401 Hz for a digital resolution of 0.68 Hz/point.

Phase-sensitive 2D NOESY spectra at 300 MHz were acquired and processed by the method of States et al. (1982). Two sets of 256 × 512 complex data matrices were collected in alternate blocks. Each t_1 value required 64 scans with a 400-ms mixing time and a 3-s relaxation delay between acquisitions. The total experimental time was 20 h. Prior to Fourier transformation 45°- and 60°-shifted sine bell functions were used in the t_2 and t_1 dimension, respectively, and zero filling in both dimensions produced a final data matrix of 1K × 1K real points. The sweep width was 1553 Hz with a digital resoluion of 1.5 Hz/point.

The 2D HOHAHA spectra at 500 MHz were obtained with isotropic mixing by the MLEV 17 method using the pulse sequence of Bax and Davis (1985):

$$90°–t_1–SL_x–(MLEV17)_n–SL_x–Acq$$

The spectra were collected with a 5-mm probe using Bruker reverse electronics. The total spin-lock mixing time was 80 ms, and a 1.0-s relaxation delay was used with a 28.6-μs 90° pulse. Phase-sensitive acquisition of the data in the ω_1 dimension was done by TPPI (Marion & Wuthrich, 1983). A 384 × 1K complex data matrix was obtained, which was zero filled in t_1 to obtain a final data matrix of 1K × 1K real points. Gaussian line broadening of 3 and 6 Hz was used in the t_2 and t_1 dimension, respectively, and the sweep width was 2404 Hz for a digital resolution of 2.35 Hz/point. The total experimental time was 10 h.

Pure-phase (TPPI) triple-quantum filtered COSY (TQF-COSY) (Piantini et al., 1982) spectra at 500 MHz were recorded with the pulse sequence

$$90°–t_1–90°_{\phi}90°_{\phi'}–90°_{\psi}90°_{\psi'}–Acq$$

with composite pulses (Muller et al., 1986). A 512 × 1K data matrix was obtained with a 6.7-μs 90° pulse and 1-s relaxation delay. The total experimental time was 8 h. Prior to Fourier transformation, 30°- and 45°-shifted sine bell functions were used in the t_2 and t_1 dimension, respectively, and zero filling in the t_1 dimension produced a final data matrix of 1K × 1K real points. The sweep width was 2404 Hz with digital resolution 2.35 Hz/point.

Exchangeable amide protons of acetamido sugars in polysaccharides (10 mg) were observed in a 90:10 mixture of H_2O and D_2O with 0.01 M trifluoroacetic acid (Bush et al., 1980) at 300 MHz by selective excitation with the Redfield 2–1–4–1–2 pulse sequence (Redfield, 1978). Acetamido proton resonances were assigned from a COSY spectrum recorded in the magnitude mode with the 90°–t_1–90°–Acq pulse sequence with appropriate phase cycling to obtain N-type peaks (Kumar et al., 1980). The strong water signal was suppressed by low-power irradiation during the 3-s relaxation delay. A constant delay of 10 ms was used before and after the mixing pulse to reduce the antiphase character of the cross-peak multiplets (Kumar et al., 1984). The experiment was carried out with a spectral width of 2600 Hz and a data set ($t_1 \times t_2$) of 256 × 1K complex points that was zero filled in t_1 to 1K × 1K. Prior to the Fourier transformation, the data were apodized by a 90°-shifted sine bell function in each dimension. The total experimental time was 10 h.

Broad-band ^1H-decoupled ^{13}C spectra were obtained at 75 MHz with a 15-kHz spectral width and 16K complex data points. The 90° ^{13}C pulse length was 12 μs, and MLEV16 decoupling was used (Levitt et al., 1982). DEPT spectra (Doddrell et al., 1982) were obtained with broad-band ^1H decoupling, a 135° ^1H pulse (115.5 μs), and a 3.4-ms delay, chosen to equal $(1/2)^1J_{CH}$, between pulses.

The heteronuclear chemical shift correlation spectra were collected in the proton-detected mode with a Bruker 5-mm inverse broad-band probe using Bruker reverse electronics. Protons were pulsed with the decoupler, while the other nuclei were pulsed with the transmitter. The pulse sequence used for the single-bond ^1H–^{13}C heteronuclear multiple-quantum correlation ($^1H[^{13}C]$HMQC) experiments was that of Bax et al. (1983). WALTZ-16 (Shaka et al., 1983) decoupling at the carbon frequency was used during acquisition to collapse proton–carbon couplings.

^1H-detected carbon–proton multiple-bond correlation spectra ($^1H[^{13}C]$HMBC) were recorded without ^{13}C decoupling during data acquisition (Bax & Summers, 1986). Modified phase cycling was used for phase-sensitive data acquisition by TPPI. A delay of 3.4 ms [$\Delta_1 = (1/2)^1J_{CH}$] was used to suppress one-bond correlations in the 2D spectrum. A delay (Δ_2) of 70 ms was used between the first two 90° ^{13}C pulses. The second 90° ^{13}C pulse applied after Δ_2 creates multiple-bond, multiple-quantum coherence. In principle, the optimum choice of Δ_2 is $(1/2)^nJ_{CH}$, where $^nJ_{CH}$ is the long-range coupling constant of interest (typically 3–9 Hz). However in practice due to the decay of ^1H magnetization during long Δ_2, a somewhat shorter value is found to be optimal. Spectra are presented in the mixed mode (Bax & Marion, 1988), absorption in f_1 (^{13}C) and absolute value in f_2 (^1H). Additional experimental details are given in the figure captions.

^1H-detected proton–phosphorus multiple-quantum correlation ($^1H[^{31}P]$HMQC) spectra were recorded with WALTZ decoupling in the ^{31}P dimension during data acquisition. The pulse sequence used was that of Bax et al. (1983), and a 64 × 1K (TPPI) data matrix was zero filled to 128 data points in t_1. There were 16 scans per t_1 value, and 1-s recycle delay was used for a total experimental time of 32 min. Four data sets were acquired with delay times of 40, 60, 80, and 120 ms. Spectra are presented in the mixed mode, absorption in f_1 (^{31}P) and absolute value in f_2 (^1H). Additional experimental details are given in the figure captions.

All the 2D data sets recorded on the NT-300 spectrometer were transferred via a high-speed parallel data link to a DEC VAX computer for processing with the FTNMR (version 5.1) program of Dennis Hare (Hare Research, Woodinville, WA). Bruker data sets were transferred to the VAX via magnetic

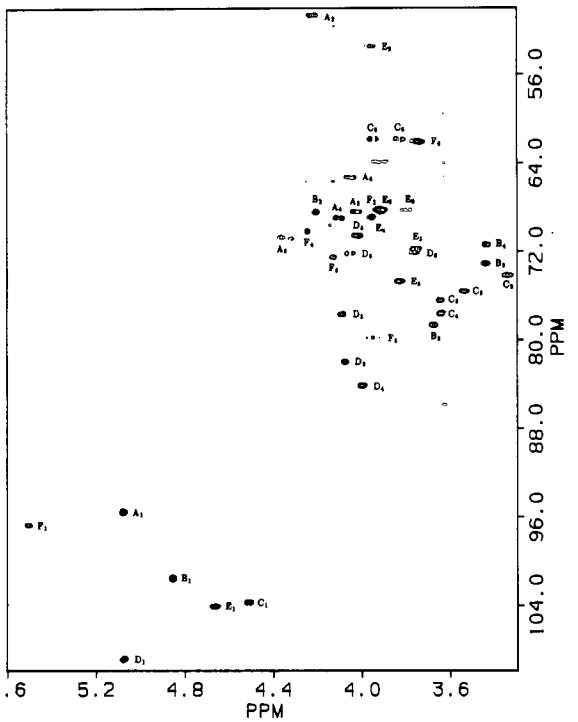

FIGURE 1: Phase-sensitive, ^{13}C-decoupled, ^{1}H-detected multiple-quantum correlation ($^{1}H[^{13}C]HMQC$) spectrum of the polysaccharide from *S. sanguis* 34 recorded at 500-MHz ^{1}H frequency. The data matrix was 512 × 1K complex points (TPPI) with 20 scans at each t_1 value. The sweep width was ±6410 Hz in f_1 and 2564 Hz in f_2. Total experimental time was 8 h. Sine bell apodization with 90° and 60° phase shifts were used in the t_1 and t_2 dimension, respectively. Zero filling was used in t_1 to obtain a 1K × 1K real matrix.

tape and the Bruker data transfer protocol in the FTNMR program.

RESULTS

Streptococcus sanguis 34 Polysaccharide. The ^{13}C NMR spectrum of the intact polysaccharide of *S. sanguis* 34 (data not shown) is consistent with the structure proposed in our previous work (Abeygunawardana et al., 1989). The spectrum shows six resolved anomeric ^{13}C resonances with that at 96.55 ppm split into a doulet by phosphorus–carbon coupling ($^{2}J_{PC}$ = 6 Hz). This resonance (F1) is identified as the anomeric carbon of the α-galactosyl phosphate moiety (C-1 of residue F). The individual residues are identified by capital letters in structure I, and we conventionally indicate ^{13}C resonance by a capital letter and a number for the carbon atom assigned. The spectrum also shows a signal at 17.67 ppm assigned to the methyl carbon resonance of β-Rha (B6) and two signals at 53.35 and 50.61 ppm characteristic of C-2 atoms of 2-acetamido-2-deoxy sugars together with resonances characteristic of carbonyl carbons at 176.02 and 175.45 ppm and methyl carbons at 23.16 and 22.98 ppm assigned to *N*-acetamido groups. Resonances at 72.06, 68.05, 65.04, 61.91, and 61.66 ppm are identified as methylene carbon signals by the DEPT sequence (data not shown). The methylene resonance at 65.04 ppm also shows splitting due to ^{31}P coupling ($^{2}J_{PC}$ = 15 Hz) and is identified as C-6 of α-D-GalNAc residue A.

The ^{13}C-decoupled ^{1}H-detected heteronuclear multiple-quantum coherence ($^{1}H[^{13}C]HMQC$) spectrum (Figure 1) shows resolved cross peaks for most of the ^{13}C–^{1}H single-bond connectivities. Correlation of H-1 of α-D-galactopyranosyl phosphate (residue F) with the ^{13}C resonance at 96.55 ppm is consistent with the previous assignment (F1) based on J_{PC} made above. Overlapping resonances at 5.068 ppm assigned to the anomeric protons of β-D-Gal*f* (D) and α-D-GalNAc (A) show correlation to well-separated ^{13}C resonances. The characteristic downfield shift of the anomeric ^{13}C resonance at 108.63 ppm suggests assignment to β-galactofuranoside (D), a proposal which is supported by other correlation data to be discussed below. The other anomeric ^{13}C resonances were assigned by direct correlation to their anomeric ^{1}H resonances.

The direct correlation for such characteristic ^{13}C resonances as the methyl carbon signals (17.67 ppm) of β-L-Rha, the C-2 carbon signals (50.61 and 53.35 ppm) of the GalNAc residues, and the unsubstituted methlene carbon resonances of β-D-Glc (61.66 ppm) and α-galactosyl phosphate (61.91 ppm) was straight forward. Although correlation peaks were observed for all the directly coupled pairs of ring carbons and protons in the HMQC spectrum, their analysis was not straight forward partly due to incomplete proton assignments in the previous studies (Abeygunawardana et al., 1989). Nevertheless, high digital resolution in the ^{1}H dimension (±0.005 ppm) enabled selection of most of the individual proton resonances and assignment of their directly coupled carbon resonances. Even in the case of closely spaced carbon resonances, assignment by direct correlation was possible because the relative order of carbon resonances in the HMQC spectrum was preserved in spite of low digital resolution (±0.1 ppm) in the ^{13}C dimension. Assignments of resonances of carbon atoms directly bonded to strongly coupled ^{1}H resonances and previously unassigned ^{1}H resonances were obtained by iterative comparison of HMQC data with the heteronuclear multiple-bond correlation ($^{1}H[^{13}C]HMBC$) spectrum. The HMBC spectrum of the *S. sanguis* 34 polysaccharide (Figure 2) shows a large number of inter- and intraresidue proton–carbon long-range connectivities. These intraresidue long-range connectivities can be used to obtain the remaining proton resonances and, hence, the complete ^{13}C assignment of the polysaccharide. The basic strategy employed in assigning HMQC data was to pick individual cross peaks (beginning with the most downfield ring proton resonance) and to assign the corresponding ^{13}C resonance on the basis of the ^{1}H chemical shifts. In this way the peaks belonging to the unassigned ^{1}H resonances can be easily identified, and chemical shift values of previously assigned proton resonances can be confirmed. For example, the resonance of C-6 of α-D-GalNAc (65.04 ppm) shows correlation to two geminal protons at 4.06 and 4.03 ppm. These two proton resonances, which were previously assigned by 1D HOHAHA at 300 MHz as 4.06 and 4.01 ppm, are less strongly coupld at 500 MHz than at 300 MHz. These revised shifts are more accurate.

The ^{1}H resonance at 4.367 ppm, which was previously assigned as H-5 of α-D-GalNAc (residue A) by means of 1D NOE (Abeygunawardana et al., 1989) shows one-bond correlation to the ^{13}C resonance at 70.50 ppm. The observation of fine coupling due to phosphorus ($^{3}J_{PC}$ = 13 Hz) in the resolution-enhanced carbon spectrum (data not shown) thus confirmed both the ^{1}H and the ^{13}C assignments. The region of 4.4–4.1 ppm in the ^{1}H dimension contains five resonances, and assignment of their directly bonded carbon atoms follows from the one-bond correlation (Figure 1) with the previously assigned ^{1}H spectrum. These carbon assignments along with complete proton chemical shifts of *S. sanguis* polysaccharide are summarized in Table I.

The ^{1}H resonances in the region between 4.1 and 4.0 ppm show direct correlation to seven ^{13}C resonances, one of which was the previously assigned to C-6 of α-D-GalNAc (residue A). Since only four protons other than the H-6's of α-D-GalNAc were previously assigned in this region, several unassigned ^{1}H resonances must be located in this chemical shift

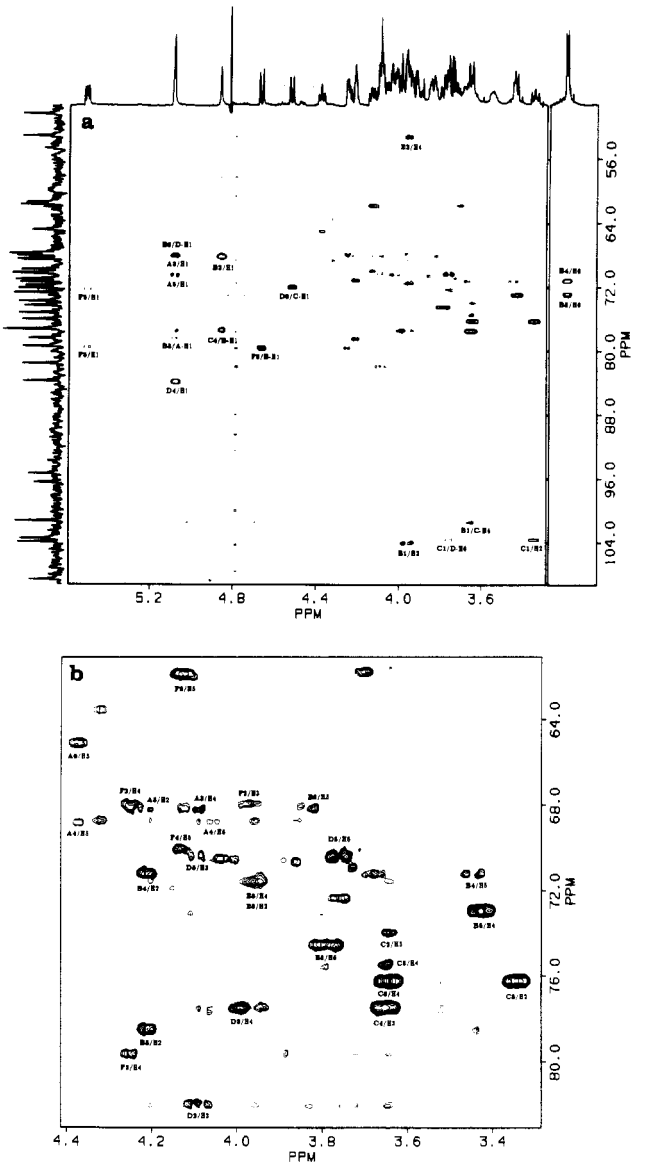

FIGURE 2: (a) ^1H–^{13}C multiple-bond correlation ($^1H[^{13}C]$HMBC) spectrum of *S. sanguis* 34 polysaccharide recorded at 500 MHz. The data matrix was 780 × 1K (TPPI) with 64 scans per t_1 value and 1.5-s relaxation delay. The spectral window was 2564 Hz in t_2 and 21 740 Hz in t_1. The delays were $\Delta_1 = 3.4$ ms and $\Delta_2 = 70$ ms. Total experimental time was 13 h. Matched apodization was used in t_2, and a 90°-shifted sine bell function was used in the t_1 dimension. Zero filling was used in t_1 to make a final data matrix of 1K × 1K real points, and the data are presented in the mixed mode, absorption in f_1 and absolute value in f_2. Ridges in f_1 were suppressed by skyline subtraction (Bax & Marion, 1988). (b) An expansion.

range. Due to the overlapping anomeric resonances and strong coupling effects at 300 MHz, assignment of H-3, H-4, and H-5 of β-galactofuranosyl residue D was not successful in the previous studies. But in the HMQC spectrum the strong coupling effects were eliminated by the low natural abundance of the ^{13}C nuclei and the large values of one-bond ^{13}C–^1H coupling constants. Therefore, it was possible to determine accurate chemical shifts of protons which were otherwise strongly coupled in conventional homonuclear experiments. The cross peak observed at 4.075 ppm (^1H) and 81.76 ppm (^{13}C) was assigned to Gal*f* H-2 and C-2 on the basis of the characteristic downfield shift of the C-2, C-3, and C-4 resonances of furanosidic sugars (Beier et al., 1980). Proton resonances at 4.09 ppm show correlation to two carbon resonances, one of which (68.83 ppm) was assigned as α-D-GalNAc C-4 (A4) by correlation to the H-4 resonance (4.085 ppm). This assignment was confirmed by the HMBC experiment reported in Figure 2, in which resonance A4 shows multiple-bond correlation to H-5 of the same residue. The other carbon resonance (77.51 ppm) and its directly coupled proton (4.087 ppm) were assigned as C-3 and H-3 of β-D-Gal*f* (residue D). This assignment was also confirmed by the HMBC experiment, in which resonance D2 shows correlation to H-3 of residue D. The methylene carbon resonance at 72.06 ppm shows correlation to two ^1H resonances at 4.05 and 3.75 ppm which were previously assigned by ^1H NOE data as Gal*f* H-6 protons (Abeygunawardana et al., 1989). The ^1H resonances near 4.01 ppm, one of which was previously assigned as α-D-GalNAc H-3, gave correlation to carbon resonances at 68.26 and 70.46 ppm. The assignment of α-D-GalNAc C-3 at 68.26 ppm was supported by the observation of long-range connectivities to H-1 and H-2 of same residue in the HMBC spectrum. The unidentified proton resonance at 4.01 ppm and its one-bond coupling partner at 70.46 ppm were asssigned as Gal*f* H-5 and C-5, respectively, by the observation of a small cross peak between the ^{13}C resonance at 70.46 ppm (D5) and the resonance assigned to H-3 of the same residue (4.087 ppm) in the HMBC spectrum. A large cross peak was also observed in HMBC between D5 and one of the H-6's (3.75 ppm) of the furanose residue. The proton resonance at 3.995 ppm gave one-bond correlation to the most downfield ring carbon resonance (83.93 ppm) and was assigned as Gal*f* H-4 on the basis of the observed long-range correlation to C-3 of same residue (D3). All these assignments of the Gal*f* resonances agreed well with a large number of long-range connectivities observed (Table II) in the HMBC spectrum to be discussed below.

In the HMQC spectrum there are four well-separated carbon resonances which showed correlation to proton resonances near 3.95 ppm. Two of these ^{13}C resonances were previously assigned as β-D-GalNAc C-2 and β-D-Glc C-6. Two other ^1H signals which have been firmly assigned at this chemical shift are α-D-Gal H-3 (3.967 ppm) and β-D-GalNAc H-4 (3.947 ppm). Assignment of α-D-Gal C-3 to 79.63 ppm was confirmed by long-range correlation to H-1 and H-4 of the same residue. This rather uncharacteristic downfield shift of α-D-Gal C-3 may be explained on the basis of the glycosylation effect (Shashkov et al., 1988) of the GalNAc*p*-β-(1→3)Gal glycosidic linkage. The remaining carbon resonance at 68.74 ppm was then assigned to C-4 of β-D-GalNAc.

The remaining methylene carbon resonance at 68.05 ppm was assigned as C-6 of the β-D-GalNAc residue by long-range correlation to H-5 of the same residue. The assignment of H-5 of any pyranoside residue with the β-galacto configuration is established by intraresidue NOE to the anomeric proton. The ^{13}C resonance at 68.01 ppm in the resolution-enhanced carbon spectrum (data not shown) shows a fine splitting due to ^{31}P–^{13}C coupling ($^3J_{PC} = 9$ Hz) and as assigned as α-D-Gal C-2. Direct correlation from the C-6 resonance of β-D-GalNAc was used to assign the methylene protons of the residue. In the HMQC spectrum α-D-Gal H-2 (3.893 ppm) and one of the H-6's (3.91 ppm) of the β-D-GalNAc residue gave an overlapping correlation peak to carbon resonances at 68.05 ppm. The other H-6 resonance (3.78 ppm) also shows one-bond correlation to the same carbon resonance. This methylene proton resonance gave long-range correlation in the HMBC spectrum to a ^{13}C resonance at 74.54 ppm. This carbon resonance in the HMQC spectrum shows correlation to its directly bonded proton resonance at 3.82 ppm, a signal assigned as H-5 of β-D-GalNAc on the basis of NOE data. The ^1H resonances of β-D-GalNAc H-3, Rha H-3 and H-6(Me), and Glc H-5 and H-2 gave well-isolated cross peaks in the HMQC spectrum,

Table I: NMR Chemical Shifts of the Polysaccharide from *S. sanguis* 34 in D_2O at 24 °C

		residue					
	assignment	α-GalNAc (A)	β-Rha (B)	β-Glc (C)	β-Gal*f* (D)	β-GalNAc (E)	α-Gal (F)
$^1H^a$	H-1	5.068	4.846	4.508	5.068	4.653	5.493 (6.9)
	H-2	4.216	4.199	3.335	4.075	3.959	3.893
	H-3	4.015	3.666	3.644	4.087	3.746	3.967
	H-4	4.085	3.434	3.639	3.995	3.947	4.241
	H-5	4.367	3.435	3.541	4.010	3.82	4.13
	H-6	4.03	1.342	3.824	3.75	3.78	3.73
	H-6′	4.06		3.943	4.05	3.91	3.73
$^{13}C^b$	C-1	95.46	101.36	103.56	108.63	103.98	96.55 (6)
	C-2	50.61	68.35	74.01	81.76	53.35	68.01 (9)
	C-3	68.26	78.63	76.27	77.51	71.61	79.63
	C-4	68.83	71.27	77.49	83.93	68.74	70.05
	C-5	70.51 (13)	72.93	75.45	70.46	74.54	72.35
	C-6	65.04 (15)	17.67	61.66	72.06	68.05	61.91
NAc	CH_3	22.98				23.16	
	CO	175.45				176.02	

[a] ^1H NMR chemical shifts are with reference to internal DSS with acetone as the internal standard (2.225 ppm downfield from DSS). Most of the ^1H chemical shift data were taken from Abeygunawardana etal. (1989). Gal*f* H3, H4, and H5 and β-GalNAc and H5 and H6's were assigned by $^1H[^{13}C]$HMQC experiment. [b] Carbon chemical shifts are with reference to internal acetone (31.07 ppm). Although the C–H connectivities were established by $^1H[^{13}C]$HMQC (±0.1 ppm), accurate chemical shifts (±0.005 ppm) were obtained from the resolution-enhanced ^{13}C spectrum at 75 MHz. J_{PH} and J_{PC} coupling constants are given in parentheses.

and the ^{13}C resonances were assigned by direct correlation. The strongly coupled resonances of H-3 and H-4 of β-D-Glc show correlation to two separate ^{13}C resonances, and Glc C-3 (76.27 ppm) was assigned by its long-range correlation in HMBC to the well-isolated H-2 resonance. Similarly in the β-L-Rha residue, the strongly coupled pair of H-4 and H-5 gave correlation to two separate carbon resonances, one of which (71.27 ppm) gave long-range correlation in HMBC to β-L-Rha H-2 and was assigned as β-L-Rha C-4.

In the HMBC spectrum (Figure 2), the intraresidue long-range correlations observed depend in a predictable way on the anomeric configuration and the relative stereochemistry of the sugar unit. Two- and three-bond coupling constants are of similar magnitude, ranging from 0 to 10 Hz depending on geometric and electronic factors. Cross peaks are generally observed between resonances for which relatively large two- and three-bond $^{13}C-^1H$ coupling constants are reported by Morat et al. (1988) for peracetylated methyl α- and β-glycosides of Gal, Glc, and Man. Since the values of $^nJ_{CH}$ depend on stereochemical and electronic factors common to O-acetylated and underivatized sugars, the values they report can be used to rationalize our observations (see Table II). The reported values of long-range $^{13}C-^1H$ coupling constants for D-mannose were used to interpret intraresidue long-range $^{13}C-^1H$ correlation data on L-Rha because these sugars have the same relative stereochemistry. As a model for the GalNAc residues, the reported values for galactose may not reflect the actual value of geminal CH couplings involving the C-2 atom due to perturbatons of the amide substituent (Cyr et al., 1978). Although the cross-peak intensity was not strictly proportional to the magnitude of the heteronuclear coupling constants involved, all the peaks except those arising from glycosidic linkages and the Gal*f* residue can be explained by reported $^nJ_{CH}$ values. However, the intensity of correlation peaks also depends on the nature of homonuclear coupling experienced by the proton of interest through its influence on the width of the ^1H multiplet. In general, a larger J_{HH} coupling for a particular proton signal leads to weaker HMBC correlation peaks for the signal (Byrd et al., 1987). In general, we observe substantial cross peaks under our experimental conditions if $^2J_{CH}$ or $^3J_{CH}$ is greater than about 3.8 Hz.

Given a complete and reliable assignment of the ^1H and ^{13}C spectra, we now proceed to evaluate the reliability of HMBC cross peaks to correctly identify the glycosidic linkages. The data of Figure 2 illustrate that all the anomeric protons except H-1 of α-galactosyl phosphate show correlation to the carbon atom across the glycosidic linkage through three-bond coupling. For the β-D-Glc and β-D-GalNAc H-1 resonances, the only observed cross peak is that across the glycosidic linkage; all the couplings of the anomeric proton to ^{13}C of the β-pyranoside ring are small. For the two α-linked residues both having the galacto configuration (residues A and F), detectable intraring cross peaks are observed to C-5 and to C-3. The overlapping anomeric proton resonances of α-D-GalNAc and Gal*f* show several long-range connectivities, including β-L-Rha C-3 and β-D-GalNAc C-6 (connectivity across the glycosidic linkage). The cross peak to A3 overlaps with that to E6. The β-L-Rha anomeric proton resonance shows correlation to β-D-Glc C-4 in addition to its own C-2 resonance.

Polysaccharide from Streptococcus sanguis J22. The discussion above demonstrates that these experimental techniques can be used to provide a rigorous and complete assignment of the ^1H and ^{13}C spectra of a complex polysaccharide and that the HMBC data are sufficient to rigorously prove the linkages. We now proceed to apply this technology to the structure of an unknown polysaccharide.

The ^1H NMR spectrum of the *S. sanguis* J22 polysaccharide in D_2O (data not shown) shows seven anomeric proton resonances including a quartet at 5.493 ppm attributable to the anomeric proton of the α-glycosyl phosphate residue. The spectrum contains signals at 2.084 and 2.053 ppm indicating two acetamido methyl groups in the polysaccharide. The presence of acetamido sugars was confirmed by amide proton resonances at 8.217 and 8.081 ppm in the ^1H NMR spectrum in H_2O. But carbohydrate analysis by reverse-phase HPLC of the benzoylated methyl glycosides of the *S. sanguis* J22 polysaccharide showed 2 mol each of Gal and Rha, 1 mol of Glc, and only 1 mol of GalNAc. Only 1 mol of GalNAc was also observed from carbohydrate analysis of the *S. sanguis* 34 polysaccharide, indicating in both cases the incomplete cleavage of the phosphate attached to C-6 of the nonreducing terminal GalNAc under the methanolysis conditions used in the carbohydrate analysis. The identity of the missing acetamido sugar in *S. sanguis* J22 was established as α-D-GalNAc on the basis of homonuclear coupling constants obtained from a double-quantum filtered COSY of the polymer in D_2O (Figure 3). The anomeric proton resonance at 5.482 ppm shows a cross peak to H-2 at 4.373 ppm in DQF-COSY. The

Table II: Summary of Intraresidue ^1H–^{13}C Long-Range Coupling Correlations Observed in the $^1H[^{13}C]$HMBC Spectrum of *S. sanguis* 34 Polysaccharide

residue	^1H resonance	^{13}C resonance	cross peak[a]	coupling constant (Hz)[b] $^2J_{CH}$	$^3J_{CH}$
α-GalOPO$_3^-$ (F)	H-1	C-3	F3/H-1		6.7
		C-5	F5/H-1		5.1
	H-3	C-2	F2/H-3	3.8	
	H-4	C-2	F2/H-4	5.5	
		C-3	F3/H-4	5.3	
	H-5	C-4	F4/H-5		5.2
		C-6	F6/H-5	<1	
β-GalNAc (E)	H-1	α-Gal C-3	F3/E-H-1		c
	H-2	C-1	E1/H-2	6.3	
		C-3	E3/H-2	6.8	
	H-4	C-2	E2/H-4		5.8
		C-3	E3/H-4	4.7	
	H-5	C-6	E6/H-5	4.7	
	H-6	C-5	E5/H-6	4.2	
β-Gal*f* (D)	H-1	β-GalNAc C-6	E6/D-H-1		c
		C-4	D4/H-1		c
	H-3	C-2	D2/H-3	c	
		C-5	D5/H-3		c
	H-4	C-3	D3/H-4	c	
	H-6	C-5	D5/H-6	c	
		β-Glc C-1	C1/D-H-6		c
β-Glc (C)	H-1	β-Gal*f* C-6	D6/C-H-1		c
	H-2	C-1	C1/H-2	5.5	
		C-3	C3/H-2	5.2	
	H-3	C-2	C2/H-3	5.3	
		C-4	C4/H-3	4.2	
	H-4	C-3	C3/H-4	4.1	
		C-5	C5/H-4	4.5	
		β-Rha C-1	B1/C-H-4		c
β-Rha (B)	H-1	β-Glc C-4	C4/B-H-1		c
		C-2	B2/H-1	8.7	
	H-2	C-3	B3/H-2	4.9	
		C-4	B4/H-2		5.9
	H-4	C-5	B5/H-4	4.1	
	H-5	C-4	B4/H-5	3.9	
	H-6	C-4	B4/H-6		c
		C-5	B5/H-6	c	
α-GalNAc (A)	H-1	β-Rha C-3	B3/A-H-1		c
		C-3	A3/H-1		5.1
		C-5	A5/H-1		6.7
	H-2	C-3	A3/H-2	8.5	
	H-4	C-3	A3/H-4	5.3	
	H-5	C-4	A4/H-5	5.2	
		C-6	A6/H-5	<1	
	H-6	C-4	A4/H-6		4.5

[a] See text for notation. Capital letters identify residue according to structure I. [b] Coupling constant data for peracetylated monosaccharides taken from Morat et al. (1988). [c] Coupling constant values are not available.

amide proton resonance at 8.081 ppm also shows a cross peak to the same resonance in water-suppressed COSY (data not shown). Similarly, the anomeric proton resonance at 5.173 ppm and the amide proton at 8.217 ppm gave cross peaks to H-2 (4.231 ppm), indicating that both amides belong to 2-deoxy-2-acetamido pyranosides. The passive coupling to H-4 seen in cross peaks between H-2 and H-3 for these residues shows that both have the galacto configuration. The absolute stereochemistry of the two GalNAc residues was determined by vacuum ultraviolet circular dichroism of the native polysaccharide, and the absolute stereochemistry of the other sugars as D-Glc, L-Rha, and D-Gal was determined from circular dichroism spectra of perbenzoylated monosaccharides (Kaluarachchi & Bush, 1989).

Incubation of this polysaccharide at 80 °C for 4 h resulted in autohydrolysis to produce a single oligosaccharide. Polysaccharides from *S. pneumoniae* which also contain internal phosphodiester linkages (teichoic acid type) are also cleaved under similar conditions (Richards et al., 1983). ^1H NMR of this oligosaccharide (data not shown) shows nine anomeric

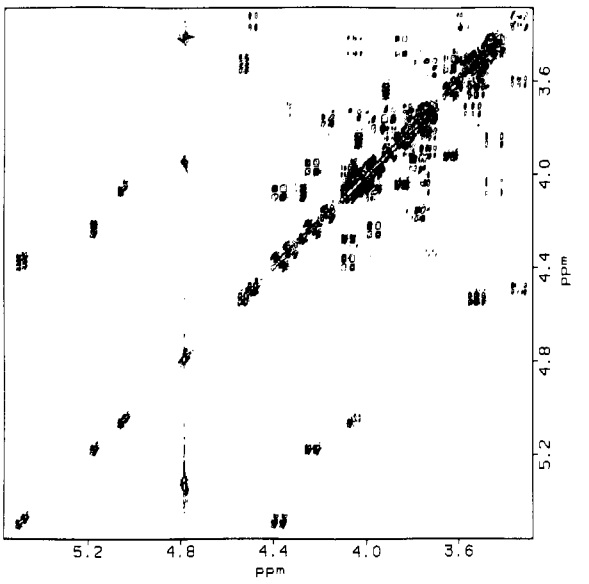

FIGURE 3: Phase-sensitive double-quantum filtered COSY spectrum of the polysaccharide from *S. sanguis* J22 at 300 MHz. The data matrix was 2 × 256 × 512 complex data points. The sweep width was ±700 Hz. Sine bell apodization with 45° and 30° phase shifts were used in the t_1 and t_2 dimension, respectively. Zero filling was used in both dimensions to obtain a 2K × 2K real matrix. Positive and negative contours are drawn with differing line thickness.

resonances, including two assigned to the α- and β-anomers of reducing terminal GalNAc and two anomeric resonances for the next sugar unit. This indicates cleavage of the α-*N*-acetylgalactosyl phosphate linkage during autohydrolysis. ^{31}P NMR of both the native polysaccharide and oligosaccharide indicates the presence of a single phosphorus atom in each, as phosphodiester (1.2 ppm, pD 5.6) and phosphomonoester (3.1 ppm, pD 5.6), respectively. These data indicate that the polysaccharide from *S. sanguis* J22 is composed of a heptasaccharide repeating unit polymerized through phosphodiester linkages and that the heptasaccharide repeating unit consists of 2 mol each of D-GalNAc, D-Gal, and L-Rha and 1 mol each of D-Glc and phosphate.

The phase-sensitive COSY spectrum (Figure 3) obtained with double-quantum filtering has several advantages over conventional COSY (magnitude mode) spectra of complex carbohydrates. The pure absorption line shapes, reduced diagonal intensity, and antiphase components within cross peaks in DQF-COSY provide a clear and accurate way to obtain chemical shift values for coupled protons. It not only provides characteristic multiplicity within the cross peak enabling identification of the particular sugar unit but also provides semiquantitative information on the coupling constants of the protons involved in the particular cross peak.

Starting from the well-separated anomeric proton resonances, ring protons of individual sugar components can be assigned from cross peaks in the 2D COSY contour map. H-1/H-2 cross peaks arising from a hexapyranose with α-D-Gal or α-D-Glc configuration (axial H-2) have a characteristic pattern with small active coupling (J_{12} = 3–4 Hz) and large passive coupling (J_{23} = 10–11 Hz). However, H-1/H-2 cross peaks arising from hexapyranoses with equatorial H-2, namely, Rha and Man, give a different pattern with the H-2 resonance having small active and passive coupling (J_{12} and $J_{23} \leq 2$ Hz) constants regardless of anomeric configuration (Altona & Hasnoot, 1984). Galacto and gluco configurations can be distinguished by the difference in their J_{34} which can be obtained either as active coupling in H-3/H-4 cross peaks or as passive coupling in H-2/H-3 cross peaks. For example, both

GalNAc residues (A and F in Figure 3) gave very characteristic H-2/H-3 cross peaks having large active (J_{23} = 11 Hz) and small passive (J_{12} and J_{34} = 3.6 Hz) couplings in both dimensions, indicating that both GalNAc residues in the *S. sanguis* J22 polysaccharide are in the α-anomeric form. The H-1/H-2 cross peak for α-D-GalNAc-1-phosphate (F) shows displacement of resonance peaks in ω_1 and ω_2 cross sections due to passive long-range coupling of ^{31}P to both resonances. Similar effects have been observed previously in the DQF-COSY spectrum of ^{113}Cd-enriched metallothionein 2 (Neuhaus et al., 1984). The four-bond coupling ($^4J_{PH} \leq 3$ Hz) to the H-2 resonance is clearly visible in the resolution-enhanced 1D proton spectrum at 500 MHz (data not shown). The occurrence of this rather unusual $^4J_{PH}$ coupling for a freely rotating system has been observed previously in aldosyl phosphates (Ogawa & Seta, 1982). As it has been reported by Hall and Malcolm (1972) that coupling through four bonds depends on the presence of a trans-antiplanar arrangement of the five atoms involved; the observation of a four-bond coupling of 2.4 Hz between the H-2 and the phosphorus atom of α-D-GalNAc-phosphate strongly indicates that the spatial arrangement of H2–C2–C1–O–P is trans-antiplanar, in agreement with the favored conformation due to the exoanomeric effect (Lemieux & Koto, 1974).

Beginning with the respective anomeric protons, resonances up to H-4 were assigned for each of the α-D-GalNAc residues in the polymer following connectivities in the ^1H COSY spectrum of Figure 3. Connectivities beyond the H-4 resonances to H-5 and two H-6's were not readily visible in the DQF-COSY spectrum due to the small J_{45} ($\leq$1 Hz). The reduced intensity is attributed to cancellation of antiphase components in the cross peak arising from small active coupling between the H-4 and H-5 resonances. Although the H-4/H-5 cross peak of α-D-GalNAc-1-phosphate (residue F) could be seen at a lower contour level, the H-4/H-5 cross peak of the other α-D-GalNAc residue (A) was obscured by spectral overlapping with more intense cross peaks. In general, extending assignments beyond H-4 protons by COSY connectivity is not practical for sugars having the galactopyranose configuration. Assignment of H-5 and H-6 resonances of the sugar residues were obtained by the TQF-COSY discussed below.

Starting with the anomeric resonance at 4.529 ppm (J_{12} = 8 Hz), the resonances up to H-4 of β-D-Gal (residue E) were assigned in the DQF-COSY spectrum. Although the chemical shifts of H-2 and H-3 in this residue are similar, the H-2/H-3 cross peak is well resolved in the spectrum due to reduced diagonal intensity. The characteristic multiplicity pattern of the H-3/H-4 cross peak with a small active coupling (J_{34} = 3.4 Hz) and large passive coupling (J_{23} = 11 Hz) established the identity of this residue as β-galactopyranose. Because of the small J_{45} coupling constant, obtaining connectivity beyond H-4 from the DQF-COSY spectrum was not possible for this residue.

The anomeric proton resonance at 4.487 ppm (J_{12} = 7.5 Hz) shows a cross peak to an H-2 resonance with partial cancellation of the central components of the cross peak indicating nearly equal J_{12} and J_{23} coupling constants. Although the cross peak between the H2 and H3 resonances is well isolated, its fine structure is distorted indicating that the H-3 and H-4 resonances of this residue are strongly coupled (Widmer & Wuthrich, 1987). These strong coupling effects precluded continued assignment by DQF-COSY, and assignment of proton resonances beyond strongly coupled pairs in the residue was obtained from data of the 2D HOHAHA experiment

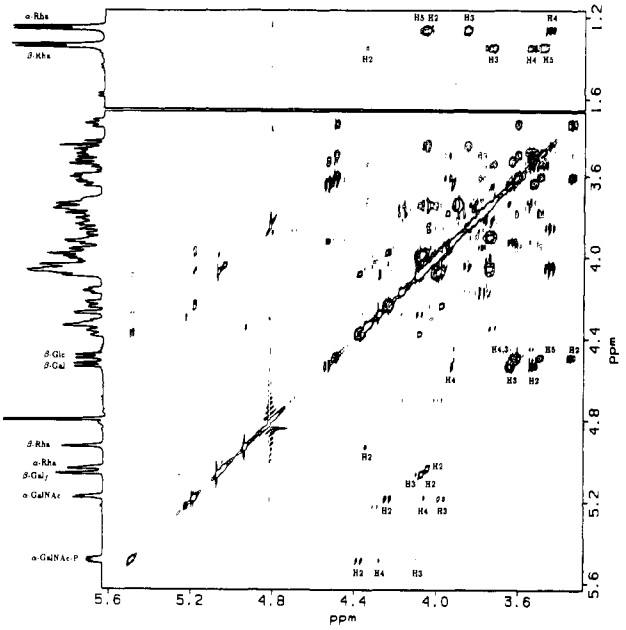

FIGURE 4: Phase-sensitive homonuclear Hartmann–Hahn spectrum of the polysaccharide from *S. sanguis* J22 at 500 MHz. The data matrix was 384 × 1K complex data points (TPPI). The sweep width was ±1202 Hz, and the spin-locking time was 80 ms. Gaussian line broadening of 6 and 3 Hz was used in the t_1 and t_2 dimension, respectively. Zero filling was used in t_1 to obtain a 1K × 1K real matrix. Normal 1D ^1H spectrum is displayed at the left side.

(Figure 4). For each diagonal peak in the 2D HOHAHA spectrum, the scalar coupled resonances in the spin system can be obtained by examining the cross section along either the f_1 or f_2 axis. The anomeric proton resonance (4.487 ppm) of this residue shows cross peaks to all the proton resonances including both H-6's. Since among the hexapyranoses present in the polysaccharide this can be possible only for sugars having the gluco configuration (large vicinal couplings among ring protons due to trans diaxial orientation), the identity of the residue was established as β-glucose, residue C. Although HOHAHA correlation from H-1 to H-6's has been observed for both α- and β-mannopyranosyl residues in high-mannose oligosaccharides by use of a relatively long spin lock time (125 ms) (Homans et al., 1987), sugars having the gluco- and mannopyranosyl configuration can be distinguished on the basis of J_{12} which is easily observed in 1D spectra or in DQF-COSY spectra. The α-anomeric protons of the two GalNAc residues (A and F) showed cross peaks to H-2, H-3, and H-4, in HOHAHA (Figure 4), as did the β-anomeric signal of Gal (residue E). The connectivity of H-1 to H-5 and further to the H-6's was not observed owing to the small scalar coupling between H-4 and H-5 for sugars having the galacto configuration.

Assignment of the ^1H resonances of the two rhamnose residues and of the second galactose residue was complicated by the small values of J_{12}. Two residues gave anomeric ^1H resonances as unresolved ($J_{12} \leq 1$ Hz) singlets at 5.036 and 4.921 ppm, and the other residue gives a signal at 5.058 ppm with J_{12} = 2 Hz. Since the anomeric proton signals for both α- and β-anomers of rhamnose have small coupling constants to the equatorial H-2 resonance, the coupling constant values cannot be used to distinguish these anomeric resonances. The anomeric resonance at 4.925 ppm shows a cross peak to H-2 (visible at lower contour level), and connectivity up to the H-4 resonance can be traced in the DQF-COSY contour map. The H-3/H-4 cross peak shows distorted multiplicity indicating strong coupling between the H-4 and H-5 resonances. Although connectivity beyond H-2 was not seen in the cross

Table III: NMR Chemical Shifts of the Polysaccharide from *S. sanguis* J22 in D_2O at 24 °C

		residue						
	assignment	α-GalNAc (A)	α-Rha (G)	β-Rha (B)	β-Glc (C)	β-Gal*f* (D)	β-Gal (E)	α-GalNAc (F)
^1H	H-1	5.173	5.036	4.921	4.487	5.058	4.529	5.482 (7.5)[c]
	H-2	4.231	4.036	4.332	3.337	4.066	3.521	4.373
	H-3	3.965	3.849	3.718	3.596	4.081	3.636	4.076
	H-4	4.056	3.445	3.537	3.605	3.983	3.919	4.272
	H-5	4.323	4.049	3.473	3.486	4.004	3.817	4.164
	H-6	3.99	1.264	1.348	3.780	3.736	3.732	3.74
	H-6′	4.06			3.947	4.046	3.898	3.79
	NAc[a]	2.053						2.084
	NH[b]	8.217						8.081
^{13}C	C-1	95.66	100.88	101.42	103.50	108.55	105.29	95.18 (6)
	C-2	50.83	71.27	72.92	73.94	81.69	71.36	49.47 (8)
	C-3	67.92	71.02	79.47	76.80	77.44	73.23	77.63
	C-4	68.81	72.66	71.67	77.96	83.82	69.52	69.36
	C-5	70.36 (6)	69.41	73.37	75.54	70.40	74.53	72.55
	C-6	65.31 (4)	17.46	17.66	61.78	72.06	68.08	61.98
NAc	CH_3	22.96						23.07
	CO	175.52						175.74

[a] Assigned by chemical shift analogy with *S. sanguis* 34 polysaccharide. [b] Data were obtained by water-suppressed COSY at 24 °C in H_2O–D_2O (90:10). [c] J_{PC} coupling constants (in parentheses) were obtained by resolution-enhanced ^{13}C spectrum at 75 MHz.

Table IV: Summary of Observed Connectivities in the NMR Spectra of *S. sanguis* J22 Polysaccharide[a]

experiment	^1H signal	α-GalNAc (A)	α-Rha (G)	β-Rha (B)	β-Glc (C)	β-Gal*f* (D)	β-Gal (E)	α-GalNAc (F)
HOHAHA	H-1	H-2,3,4	H-2,3 (w)	H-2	H-2,3,4,5,6,6′	H-2,3,4	H-2,3,4	H-2,3,4
	H-5	H-6,6′			H-6,6′			H-4,6,6′
	H-6′		H-2,3,4,5	H-2,3,4,5				H-5
NOESY	H-1	H-2	H-2	H-2,3,5	H-3,5	H-2	H-3,5	H-2
		GH-1[b]	BH-2[b]	CH-4[b]	DH-6,6′[b]		FH-3[b]	
		BH-2[b],3[b] (w)						
TQF-COSY	H-6′	H-5,6			H-6	H-5,6	H-5,6	H-5,6
$^1H[^{13}C]$HMBC	H-1	A3, A5, B3 (w)[b]	G3, G5, B2[b]	B2, C4[b]	D6[b]	D4, E6[b]	F3[b]	F3, F5
	H-2	A3	G3, G4	B1, B3, B4, G1[b]	C1, C3	D3 (w)	E3	F3
	H-3	A2	G4		C2, C4	D2, D5	E2	F2 (w)
	H-4	A2, A3	G3, G5, G6	B3, B5, B6	C3, B1[b]	D3, D5	E2, E3	F2, F3
	H-5	A4, A6	G4	B4			E6	F4, F6
	H-6		G4, G5	B4, B5		D5	E5	
	H-6′							F5 (w)
$^1H[^{31}P]$HMQC	H-1							P
	H-2							P (w)
	H-6,6′	P						

[a] Except in the case of strong coupling, all protons showed cross peaks in DQF-COSY for vicinal and geminal coupling partners. All protons showed signals arising from one-bond correlations with their attached carbon atoms. (w) refers to a weak cross peak. [b] Interresidual connectivities.

section taken through the anomeric resonance in the HOHAHA spectrum of Figure 4, connectivity up to the same H-2 resonance from the well-resolved methyl proton resonance (H-6 at 1.348 ppm) was clearly visible in the 2D HOHAHA spectrum. The same strategy was used to assign the anomeric ^1H resonance at 5.036 ppm to the other rhamnose, residue G. The anomeric configuration of this residue was determined to be α from the 2D NOESY spectrum (Figure 5) which shows NOE connectivity from H-1 to H-2 as the only intraresidue NOE. For the other rhamnose residue (B), the data of Figure 5 show intraresidue NOE connectivity from H-1 to H-2, H-3, and H-5 (Table IV) indicating the β-anomeric configuration. The anomeric configuration assignments based on intraresidue NOE connectivities of the two rhamnose residues are in good agreement with the correlation of the chemical shifts of H-5 and H-6 with the anomeric configuration proposed by Laffite et al. (1978). The DQF-COSY spectrum (Figure 3) shows the high-field methyl resonance (H-6 of α-L-Rha at 1.264 ppm) to be correlated with H-5 at 4.049 ppm and the methyl group H-6 of β-L-Rha at 1.348 ppm to be correlated with H-5 at 3.473 ppm, in agreement with the behavior expected of α- and β-L-Rha*p*, respectively (Jones, 1985).

The anomeric resonance at 5.058 ppm (J_{12} = 2 Hz) shows direct correlation to the ^{13}C resonance at 108.55 ppm in the

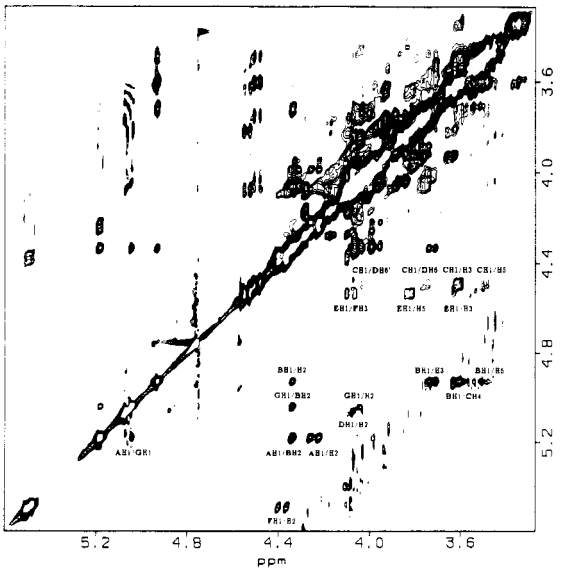

FIGURE 5: Phase-sensitive NOESY spectrum of the polysaccharide from *S. sanguis* J22 at 300 MHz. The data matrix was 2 × 256 × 512 complex data points. The sweep width was ±776 Hz, and the mixing time was 400 ms. Sine bell apodization with 60° and 45° phase shifts were used in the t_1 and t_2 dimension, respectively. Zero filling was used in both dimensions to obtain a 1K × 1K real matrix.

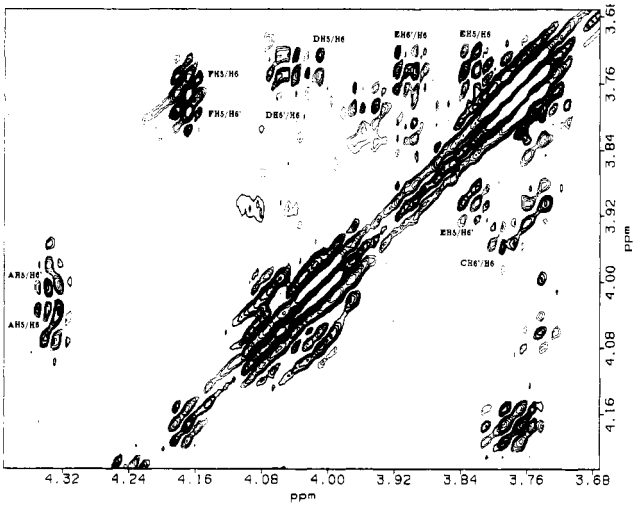

FIGURE 6: Phase-sensitive triple-quantum filtered COSY (TQF-COSY) spectrum of the polysaccharide from *S. sanguis* J22 at 500 MHz. The data matrix was 512 × 1K complex data points (TPPI). The sweep width was ±1202 Hz. Sine bell apodization with 45° and 30° phase shifts were used in the t_1 and t_2 dimension, respectively. Zero filling was used in both dimensions to obtain a 1K × 1K real matrix. Positive and negative contours are drawn with differing line thickness.

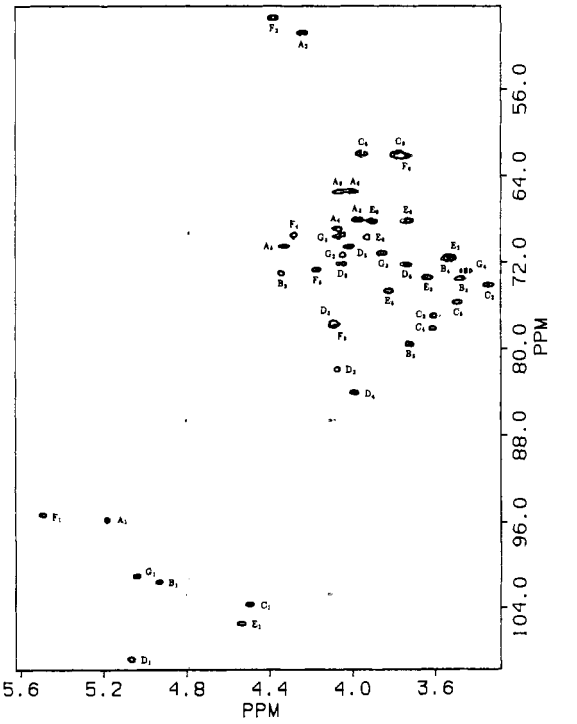

FIGURE 7: Phase-sensitive, ^{13}C-decoupled, ^1H-detected multiple-quantum correlation ($^1H[^{13}C]$HMQC) spectrum of the polysaccharide from *S. sanguis* J22 recorded at 500-MHz ^1H frequency. The data matrix was 512 × 1K complex (TPPI) with 20 scans at each t_1 value. The sweep width was ±6250 Hz in f_1 and 2604 Hz in f_2. Total experimental time was 8 h. Sine bell apodization with 90° and 60° phase shifts was used in the t_1 and t_2 dimension, respectively. Zero filling was used in T_1 to obtain a 1K × 1K real matrix.

HMQC spectrum (Figure 7) indicating that the remaining galactose residue (D) is in the β-furanosidic form (Beier et al., 1980). The anomeric ^1H resonance gave asymmetric cross peaks in the DQF-COSY spectrum (Figure 3) indicating that the H-2 and H-3 resonances are strongly coupled. Connectivity from H-1 to H-4 could be obtained in the 2D HOHAHA spectrum. Wherever possible, proton chemical shift values obtained by the 2D HOHAHA method for strongly coupled resonances were further refined by the HMQC experiment.

The triple-quantum filtered COSY (TQF-COSY) spectrum of the polysaccharide from strain J22 (Figure 6), which gives cross peaks only for the systems having three (or more) mutually coupled spins, shows cross peaks for most of the H-5, H-6, and H-6′ spin systems including one for the Gal*f* residue. As expected, no cross peaks were detected for the two Rha residues between H-5 and the methyl group (Piantini et al., 1982). In TQF-COSY there is usually a central peak consisting of several in-phase components whereas in DQF-COSY the inner components have antiphase structures. Although these antiphase structures in DQF-COSY result in increased resolution and more accurate *J* values, partial cancellation can occur in mutually coupled ABX-type spin systems where the A and B resonances are strongly coupled. This is the often the case for sugar residues for which the two H-6 protons are close in chemical shift. Since TQF-COSY also simplifies the spectrum by filtering out all the cross peaks not arising from three mutually coupled spins, it is therefore the preferred technique for assigning the H-5 and the two H-6's of common sugars. Phase-sensitive TQF-COSY also provides information about the sign of the coupling constants involved in the particular cross peak. The sign of the central signal contribution in odd-quantum filtered spectra recorded with low digital resolution depends on the sign of the product of the coupling constants to the additional MQ-active spin (Muller et al., 1986). This can be exploited to distinguish between vicinal and geminal cross peaks in low-resolution spectra, since all the geminal ^1H–^1H coupling constants in sugars are negative and all the vicinal couplings are positive. Consequently, all the H-6/H-6′ cross peaks in TQF-COSY have positive centers in Figure 6 since passive vicinal coupling ($^3J_{5,6}$) constants are of positive sign. Vicinal cross peaks of H-5 and H-6 fragments in TQF-COSY on the other hand have a negative center. Unexpected features in Figure 6 include the H-5/H-6 cross peaks of β-D-Glc (residue C) which are strongly attenuated in TQF-COSY. This absence of particular cross peaks in TQF-COSY is probably due to the disappearance of one or more couplings to the MQ-active spins. Therefore, one must exercise care when drawing conclusions based on the absence of cross peaks in TQF-COSY.

The merits of TQF-COSY can be demonstrated by the assignments of the H-5 and H-6 resonances of the nonreducing terminal α-GalNAc residue (A). Although the H-5 resonance can be seen in resolution-enhanced 1D spectra, H-5/H-6 cross peaks are greatly attenuated in the DQF-COSY spectrum due to the destructive interference of the overlapping cross peaks of two sets each of H-5/H-6 and H-5/H-6′ split by the ^{31}P–^1H long-range couplings. Because of cross-peak symmetry along the chemical shift axes, such interferences are less probable in the TQF-COSY spectrum. Although the H-5 (4.004 ppm) and H-6 (4.046 ppm) resonances of Gal*f* (residue D) are closely spaced, cross peaks to H-6′ (3.736 ppm) can be distinguished by the sign of center components. Similarly, all the TQF-COSY cross peaks were assigned for each of the three spin systems.

The separate problem of assignment of these H-5 and H-6 resonances to individual sugar residues was solved by a variety of methods which included 2D NOESY, 2D HOHAHA, and $^1H[^{13}C]$HMBC (Figure 8) experiments. For the β-galactose residue, intraresidue NOESY cross peaks between H-1 and H-3 and H-5 (Figure 5) were used to identify the H-5 and H-6's with the correct anomeric ^1H resonance. Although NOESY was not useful for the identification of H-5 of the α-D-GalNAc residues, connectivity from H-4 to H-5 of reducing terminal α-D-GalNAc-phosphate (residue F) was observed in both 2D HOHAHA and NOESY spectra. Because

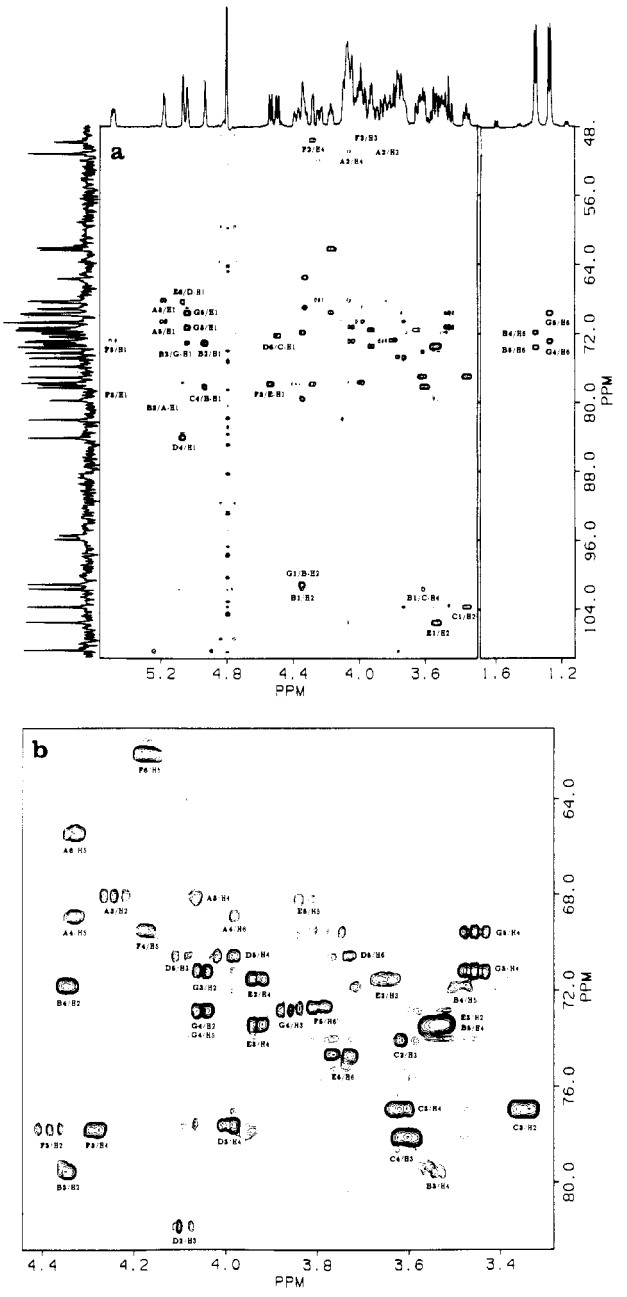

FIGURE 8: (a) ^1H–^{13}C multiple-bond correlation ($^1H[^{13}C]$HMBC) spectrum of *S. sanguis* J22 polysaccharide recorded at 500 MHz. The data matrix was 256 × 1K (TPPI) with 80 scans per t_1 value and 1.5-s relaxation delay. The spectral window was 2604 Hz in t_2 and 12 500 Hz in t_1. The delays were $\Delta_1 = 3.4$ ms and $\Delta_2 = 70$ ms. Total experimental time was 12 h. Matched apodization was used in t_2, and a 90°-shifted sine bell function was used in the t_1 dimension. Zero filling was used in t_1 to make a final data matrix of 1K × 1K real points, and the data are presented in the mixed mode, absorption in f_1 and absolute value in f_2. Ridges in f_1 were suppressed by skyline subtraction (Bax & Marion, 1988). (b) An expansion.

of the overlapping chemical shifts of the H-4 and H-6 resonances of the other α-D-GalNAc residue (A), the cross peaks between H-4 and H-5 observed in HOHAHA and NOESY did not provide a conclusive assignment. Connectivity between H-4 and H-5 of α-galacto sugars can be obtained more rigorously by long-range coupling correlation between H-1 and C-5, which is generally observed in HMBC spectra to be discussed below. The remaining H-5, H-6, and H-6′ subsystem was assigned to the Gal*f* residue (D) by HMBC correlation between Gal*f* C-5 and H-3 of the same residue. The complete proton assignments for the *S. sanguis* J22 polysaccharide are summarized in Table III.

The 2D NOESY spectrum (Figure 5) shows several cross peaks between ^1H on different sugar residues in addition to the intraresidue NOE connectivities discussed above (see Table IV). Prominent features of the NOESY spectrum of this polymer are the somewhat unusual observation of cross peaks between the anomeric resonances of residues A and G (α-D-GalNAc H-1 and α-L-Rha H-1) and observation of cross peaks between β-L-Rha H-2 and three anomeric resonances (α-D-GalNAc, α-L-Rha, and β-L-Rha). These results indicate the close proximity of residues A, B, and G. The anomeric proton resonance of α-D-GalNAc (residue A) also shows an NOE cross peak to H-2 and a weak cross peak to H-3 of β-L-Rha, whereas α-D-GalNAc-P H-1 (residue F) shows an NOE cross peak only to its H-2 resonance. Similarly, the β-D-Gal*f* anomeric resonance shows a cross peak to its H-2 resonance and no interresidue NOE cross peaks. Interresidue NOE cross peaks from β-L-Rha H-1 to β-D-Glc H-4 and H-5 resonances are observed, in addition to the intraresidue NOE's discussed above. The anomeric resonance of the β-D-Gal residue shows an interresidue NOE to α-D-GalNAc-P H-3 (residue F) in addition to the cross peaks to its own H-3 and H-5 resonances. β-D-Glc H-1 also shows interresidue NOE cross peaks to the H-6 protons of the Gal*f* residue and intraresidue NOE's to H-3 and H-5. Although it is possible to deduce sequence assignments for certain types of linkages from NOE connectivities (see Discussion), no attempt was made to obtain the linkages of the heptasaccharide from NOE's. The heptasaccharide sequence was instead obtained from observed long-range ^{13}C–^1H correlations across the glycosidic linkage by the HMBC experiment discussed below.

The normal ^{13}C spectrum of the *S. sanguis* J22 polysaccharide (data not shown) shows seven anomeric carbon resonances at 108.55, 105.29, 103.50, 101.42, 100.88, 95.66, and 95.18 ppm. In an expanded spectrum, the signal al 95.18 ppm shows ^{31}P–^{13}C coupling ($^2J_{PC} = 6.0$ Hz) and is identified as the anomeric carbon resonance of residue F. The spectrum also shows resonances at 17.66 and 17.46 ppm expected for two methyl carbon atoms of the rhamnose residues. Two signals at 50.83 and 49.47 ppm together with other characteristic resonances for *N*-acetamido groups (175.74 and 175.52 ppm for the carbonyl carbon and 23.07 and 22.96 ppm for methyl carbons) are consistent with the presence of two 2-*N*-acetamido-2-deoxygalactosyl residues in the repeating structure. The carbon resonance at 49.47 ppm shows splitting due to phosphorus long-range coupling ($^3J_{PC} = 8$ Hz) and is assigned as C-2 of α-D-GalNAc-phosphate, residue F. Five methylene carbon resonances at 72.06, 68.08, 65.31, 61.98, and 61.78 ppm are distinguished by the DEPT experiment (data not shown). As in the case of the *S. sanguis* 34 polysaccharide, the ^{13}C spectrum of the *S. sanguis* J22 polymer also contains a methylene resonance which shows ^{31}P coupling (65.31 ppm, $J_{PC} = 4$ Hz), suggesting a phosphodiester linkage to C-6 of a hexose.

The HMQC spectrum of *S. sanguis* J22 (Figure 7) shows resolved correlation peaks for most of the ^{13}C–^1H single-bond connectivities. The most downfield anomeric carbon resonance (108.55 ppm) shows correlation to a proton resonance at 5.05 ppm indicating that the Gal*f* residue indeed has the β-anomeric configuration. Other anomeric carbon resonances were assigned by correlation to their directly bonded protons.

The strategy used in assigning the ^{13}C spectrum of this polymer was the same as that for the *S. sanguis* 34 polysaccharide discussed above. More complete ^1H assignments and a lesser number of closely spaced ^1H resonances, with a chemical shift difference less than the digital resolution in the

proton dimension, made the assignments from the HMQC spectrum of the *S. sanguis* J22 polymer simpler than that of the strain 34 polysaccharide.

^{1}H resonances between 4.4 and 4.1 ppm show one-bond correlation to six well-resolved carbon resonances, one of which (49.47 ppm) shows fine splitting due to phosphorus couplings and shows correlation to H-2 of α-D-GalNAc-phosphate, residue F. Although H-5 of α-D-GalNAc residue A at 4.323 ppm gave a resolved cross peak in tthe HMQC spectrum, the ^{13}C assignment was not straightforward due to overlap of two resonances (70.36 and 70.40 ppm) in the ^{13}C dimension. But in the resolution-enhanced ^{13}C spectrum, the resonance at 70.36 ppm was split by ^{31}P–^{13}C long-range coupling ($^3J_{PC}$ = 6 Hz). This carbon resonance was assigned to α-D-GalNAc C-5 on the basis of observed P–C coupling to C-6 of the residue, as discussed below. Other carbon resonances were assigned from direct correlation to respective ^{1}H resonances (see Figure 7).

Proton resonances at 4.081 (Gal*f* H-3) and 4.076 (residue F, α-D-GalNAc-P H-3) ppm gave overlapping correlation peaks due to similar chemical shifts of the correlated ^{13}C resonances at 77.44 and 77.63 ppm. The ^{13}C resonance at 77.63 ppm was assigned to the α-D-GalNAc-P C-3 (F3) resonance on the basis of fine structure in the cross peak along the proton dimension in this phase-sensitive HMQC experiment which preserves the ^{1}H line shape very well. These assignments were supported by observed long-range correlation peaks (α-D-GalNAc-P C-3/H-4 and β-D-Gal*f* C-3/H-4) in the HMBC spectrum (Figure 8). Six proton resonances in the region between 4.07 and 4.03 ppm show correlation to six carbon resonances, two of which were identified as methylene carbons by the DEPT experiment. The ^{13}C resonance at 65.31 ppm ($^2J_{PC}$ = 4 Hz) shows correlation to both H-6 resonances of α-D-GalNAc (A) (4.06 and 3.99 ppm). The remaining methylene carbon resonance at 72.06 ppm was assigned as C-6 of β-D-Gal*f* residue D by correlating to H-6 at 4.046 ppm. This resonance also shows a correlation peak to H-6′ (3.736 ppm) of β-D-Gal*f*. Assignment of these methylene protons allowed the assignment of Gal*f* C-2 (D2 at 81.69 ppm) and α-D-GalNAc C-4 (A4 at 68.81 ppm) by direct correlation to protons at 4.066 and 4.056 ppm, respectively. The two ^{1}H resonances at 4.049 and 4.036 ppm (α-L-Rha H-5 and H-2) were correlated with ^{13}C resonances at 69.41 and 71.27 ppm, respectively. The C-5 resonance of this residue also shows long-range correlation in the HMBC spectrum to the methyl resonance at 1.264 ppm confirming this assignment. The resonances of Gal*f* C-5 and C-4 and of C-3 of α-D-GalNAc residue A were assigned by correlation in the HMQC spectrum to their directly bonded proton resonances. One of the H-6 resonances (3.947 ppm) of the β-D-Glc residue shows correlation in HMQC to the methylene carbon resonance at 61.78 ppm. The cross peak between this ^{13}C resonance and the other H-6 (3.780 ppm) was partially overlapping with the large cross peak between the methylene protons (3.74 and 3.79 ppm) and C-6 (61.98 ppm) of α-D-GalNAc-P residue F. The other methylene carbon resonance (68.08 ppm) was assigned by correlation to the β-D-Gal H-6 proton resonances at 3.732 and 3.898 ppm. Similarly, β-D-Gal C-4, C-5, and C-3, α-D-GalNAc-P C-3, and β-L-Rha C-3 were assigned by direct correlation to ^{1}H resonances whose assignment depends only on ^{1}H correlation. As was the case for the polysaccharide from *S. sanguis* 34, the resonance assigned to β-L-Rha C-3 shows a large downfield shift, consistent with a 3-substituted residue. The strongly coupled resonances of H-3 and H-4 of β-D-Glc are correlated in HMQC with ^{13}C resonances at 76.80 and 77.96 ppm. The former resonance shows long-range correlation to β-D-Glc H-2 confirming the assignment of β-D-Glc C-3 at 76.80 ppm. Because of the small reported value of the three-bond coupling constant ($^3J_{H2/C4}$ = 1.0 Hz), no long-range correlation is expected between β-D-Glc H-2 and C-4, and none was observed for the β-D-Glc residues in either polysaccharide (Figure 2 and Table II). Partially overlapping cross peaks arising from β-L-Rha C-4/H-4 and β-D-Gal C-2/H-2 precluded assignment of these ^{13}C resonances from the HMQC spectrum. The problem posed by similar chemical shift values in both dimensions can be resolved in the ^{1}H dimension by observing long-range correlation to these ^{13}C resonances in the HMBC spectrum. The ^{13}C resonance at 71.67 ppm shows long-range correlation to the resonances assigned to β-L-Rha H-2 (4.332 ppm) and H-5 (3.473 ppm), whereas the resonance at 71.36 ppm shows correlation to that assigned to β-D-Gal H-4 (3.919 ppm). The remaining ^{13}C resonances were assigned as β-D-Glc C-5 and C-2, α-L-Rha C-4 and C-6, and β-L-Rha C-5 and C-6 by one-bond correlation with the respective ^{1}H resonances. The complete ^{13}C assignment of the *S. sanguis* J22 polysaccharide is summarized in Table III.

In the HMBC spectrum (Figure 8), all the anomeric protons except H-1 of α-D-GalNAc-P (residue F) show correlation to the aglycon carbon atom through $^3J_{CH}$ coupling across the glycosidic linkage. Figure 8 also shows a large number of intraresidue long-range correlations through $^2J_{CH}$ and $^3J_{CH}$ couplings. Relatively few correlations were observed between the aglycon ^{1}H resonance and the glycosidic ^{13}C resonance. All these connectivities are summarized in Table IV. α-D-GalNAc H-1 shows long-range correlation to C-3 and C-5 resonances and β-L-Rha C-3 (79.47 ppm). The cross peak between α-D-GalNAc H-1 and β-L-Rha C-3 shows connectivity across the glycosidic linkage, indicating the GalNAc*p*-α-(1→3)Rha*p* linkage in the heptasaccharide. The anomeric proton resonance of the β-D-Gal*f* residue shows interresidue connectivity to β-D-Gal C-6 (68.08 ppm), in addition to its own C-4 resonance, indicating the Gal*f*-β-(1→6)Gal linkage in the repeating unit. Three correlation peaks from the H-1 resonance of α-L-Rha are observed in the HMBC spectrum, one of which is to β-L-Rha C-2 (at 72.92 ppm). The other two ^{13}C resonances were identified as intraresidue connectivities to C-3 and C-5 resonances, consistent with the relatively large values of $^3J_{CH}$ coupling constants reported for α-mannosyl derivatives (Morat et al., 1988). The anomeric proton of β-L-Rha shows interresidue correlation to β-D-Glc C-4 and intraresidue correlation only to C-2. The β-anomeric proton resonances of both the β-D-Gal (4.529 ppm) and the β-D-Glc (4.487 ppm) residues show connectivities only across the glycosidic linkages to α-D-GalNAc-P (F3) and β-D-Gal*f* (D6), respectively.

The correlation experiments described above permit the assignment of all the ^{1}H and the ^{13}C resonances and define all the glycosidic linkages. The position of the phosphodiester linkage is suggested by the ^{31}P scalar couplings observed in the ^{1}H and ^{13}C spectra. Splittings due to ^{31}P were observed in the ^{1}H DQF-COSY and the 1D ^{1}H spectra for the H-1 and H-2 resonances of α-GalNAc residue F. ^{31}P splittings were observed in the resolution-enhanced ^{13}C spectrum of resonances F1, F2, A5, and A6. Although ^{31}P–^{13}C couplings observed in ^{13}C spectra are often used to determine phosphodiester linkages (Egan, 1980), ambiguities could arise from spectral overlapping in the ^{13}C spectrum and from the similarity in the magnitudes of $^2J_{PC}$ and $^3J_{PC}$, suggesting that a more general approach might be desirable. ^{31}P–^{1}H scalar coupling correlation may be detected by 2D correlation either by ^{31}P de-

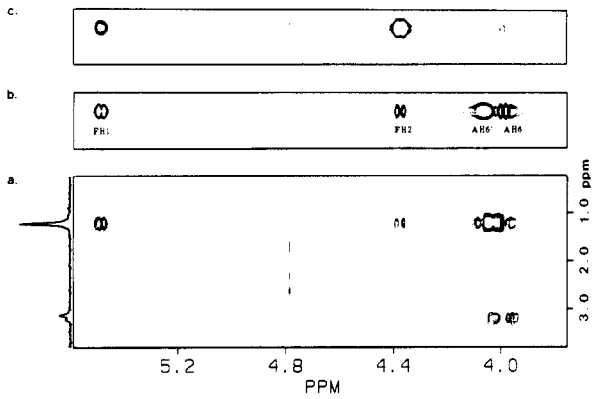

FIGURE 9: ^{31}P-decoupled, ^{1}H-detected multiple-quantum correlation (^{1}H[^{31}P]HMQC) spectrum of *S. sanguis* J22 polysaccharide. Data matrices were 64 × 1K complex points (TPPI) with 16 scans per t_1 value and a 1-s relaxation delay. The delay values were Δ = 60 ms in (a), Δ = 80 ms in (b), and Δ = 120 ms in (c). Total measurement time for each spectrum is 32 min. Shifted sine bell apodization of 60° in t_2 and of 90° in t_1 was used. Data were zero filled in t_1 for a final data matrix of 128 × 1K real points. Spectra are presented in the mixed mode, absorption in f_1 and absolute value in f_2. Normal 1D ^{31}P spectrum at left of (a) shows the extent of autohydrolysis of the polymer phosphodiester (1.2-ppm ^{31}P shift) to give monoester peak at 3.1 ppm.

tection (Fu et al., 1988) or by ^{1}H detection (Williamson & Bax, 1988; Byrd et al., 1986, 1987). Figure 9 shows a series of ^{1}H-detected ^{1}H[^{31}P]HMQC spectra of the *S. sanguis* J22 polysaccharide at different delay times (Δ), chosen to be approximately $(1/2)^{n}J_{PH}$ to cover a range of coupling constants of 4–8 Hz. The data show correlation between the ^{31}P signal at 1.2 ppm and the H1 and H2 resonances of α-GalNAc residue F and the two H6 resonances of α-GalNAc residue A confirming the linkage connecting the heptasaccharide repeating units.

Discussion

The combination of the long-range coupling correlation data of ^{1}H to ^{13}C and ^{31}P with the complete ^{31}C and ^{1}H resonance assignment led to covalent structure II for the repeating subunit of the polysaccharide from the cell wall of *S. sanguis* J22. The assignment of the stereochemistry and the linkage analysis were done without methylation analysis and depend almost exclusively on NMR methods.

structure II

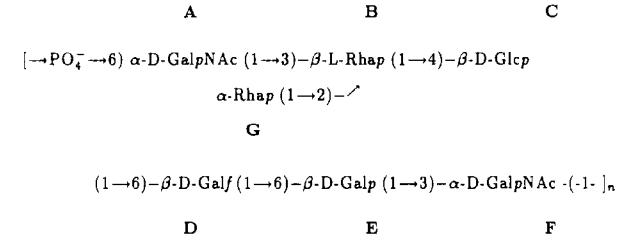

This work has shown that it is practical to deduce a complete, rigorous assignment of the complete ^{1}H and ^{13}C spectra of a polysaccharide of considerable complexity. Although the heptasaccharide repeating subunit of *S. sanguis* J22 polysaccharide poses a relatively difficult problem in structure determination with differing anomeric pyranosides and furanosides and phosphodiester linkages, the complete resonance assignment and structure determination presented few difficulties because of the redundancy provided by the multitude of different NMR methods used. If difficulties in the interpretation are encountered due to small values of coupling constants or to unfortunate overlap of chemical shifts, then there are often alternative methods for the assignment. It would appear that this approach could be effective on a carbohydrate of greater size and complexity. Polysaccharides of some other strains of *S. sanguis* having have more challenging structures which are now under study in our laboratory will serve as a more rigorous test of just how far this method of assignment can be extended.

Given a carbohydrate analysis by some chromatographic method such as the HPLC technique used in this work, the NMR data can be correlated with the analytical data to yield an unambiguous identification of each sugar residue in the NMR assignment. Measured values of $^{3}J_{HH}$ from the DQF COSY spectrum can be used to identify axial and equatorial protons and thus the stereochemical configuration as well as the anomeric configuration of the pyranoside units. 6-Deoxy sugars can be identified by the characteristic methyl group resonances which may be correlated with the main spin system of the ring. Acetamido sugars can be identified by their amide proton resonance which can then be correlated with the rest of the ring spins. It is not clear from this work how effective this approach would be in a structure containing several different furanoside sugars, but the identification of the single galactofuranoside residue in the *S. sanguis* polysaccharides was straightforward.

Given the complete ^{1}H and ^{13}C assignments for the polysaccharide, the linkages can be completely assigned with data of the HMBC spectrum. This is an attractive alternative to such methods of linkage analysis as methylation which requires a difficult chemical protocol presenting many steps at which failure can occur. Although ^{1}H NOESY has been proposed for linkage analysis in oligosaccharides, the dependence of NOESY cross peaks on the conformation of the glycosidic linkage presents some fundamental difficulties. In a completely new structure, it is unlikely that much will be known about the conformation of the glycosidic linkage, and a linkage analysis method more rigorous than NOESY may be needed. In the J22 problem for example, NOESY between the resonances of residues A, B, and G would be difficult to interpret in a straightforward and rigorous way. The glycosidic linkage of the Gal*f*-β-(1→6) residue (D) to GalNAc in strain J22 and to β-Gal in the polymer from strain 34 was not detected in the NOESY spectra. The presence of HMBC cross peaks which depend on bond connectivity provide a primary method of linkage analysis. In this work cross peaks were found between the anomeric proton resonances and the aglycon carbon atom resonances for all the linkages. It is possible that for some glycosidic linkages the conformation would be such that the glycosidic dihedral angle ϕ, upon which this coupling constant depends, might adopt a value for which $^{3}J_{CH}$ is small and the correlation could not be detected. In that case, it is possible that the glycosidic dihedral angle ψ might adopt a value such that a large coupling correlation might be observed between the anomeric ^{13}C resonance and the ^{1}H resonance of the aglycon proton (see Table II). At present the values of the long-range ^{13}C–^{1}H coupling constants across glycosidic linkages are poorly understood, and studies are now underway in our laboratory to measure these *J* values (Z. Y. Yan, unpublished results). Although it might appear that overlapping anomeric ^{1}H resonances, such as those of α-GalNac and β-Gal*f* (residues A and D) in the polysaccharide from *S. sanguis* 34, could prevent reliable linkage assignment by HMBC, this obstacle is not insurmountable. These anomeric ^{1}H chemical shifts depend on temperature, and their signals do not overlap in spectra recorded at a higher probe temperature (McIntire et al., 1987). For cases in which accidental degeneracy cannot

be removed by changing temperature, spectra may be recorded in Me_2SO or in pyridine, solvents which strongly influence carbohydrate ^1H chemical shifts (Rao & Bush, 1988).

The most difficult step in our proposed structure determination protocol is the complete resonance assignment of the spectrum. A rigorous assignment should rely primarily on coupling correlation in preference to NOE, since the former effect depends on chemical bonds rather than spatial proximity. The procedure we have described involves only a very limited use of NOESY spectra, the most important being the intraresidue NOE in pyranosides of known ring conformation. In most sugar rings the correlation of ^1H along the chain of spins is effective and provides an excellent starting point for the complete assignment (Bush, 1989). There are two serious obstacles which can prevent rigorous assignments by this method. First, the problem of strong coupling places COSY cross peaks close to the diagonal and prevents reliable tracing of connectivity. Several examples of strong coupling which were encountered in the spectra of these two polysaccharides were solved with the help of HOHAHA spectroscopy, which gives cross peaks far from the diagonal even for strongly coupled peaks (Bush, 1989). A second problem which prevents J correlation of ^1H in the ring is a small value of the vicinal ^1H coupling constants ($J \leq 1$ Hz). For example in sugars with the mannose configuration, exemplified by the rhamnose residues in this problem, $J_{H1/H2}$ and $J_{H2/H3}$ are small. Nevertheless, ^1H COSY and HOHAHA data proved adequate for reliable assignment. A more difficult case is that of sugars with the galacto configuration for which $J_{H4/H5}$ is less than 0.5 Hz. Although it is not difficult with ^1H COSY and HOHAHA data to assign H-1 through H-4 for these sugars, assignment of H-5 and H-6 may be difficult if the generally weak cross peak between H-4 and H-5 does not appear in a region of the 2D spectrum which is free from noise. Identification of individual spin systems of H-5 and H-6 can be done by TQF-COSY, but this method does not provide correlation of the spin system with the rest of the sugar ring. For sugars having the β-galacto configuration, intraresidue NOE gives strong cross peaks between H-1 and H-5 which firmly establishes this correlation, but for sugars with the α-galacto configuration no such NOESY cross peaks are observed. For the latter case one may rely on HMBC data because there are large long-range $^3J_{CH}$ and readily observable cross peaks between H-1 and C-5. The latter resonance is readily correlated with the H-5 and H-6 resonances in the heteronuclear correlation experiments.

The assignment of the ^1H resonances of furanosides is a more difficult problem which has not received much attention in the literature. For the β-galactofuranoside which occurs in these two polymers, strong coupling of the furanoside protons H-2, H-3, H-5, and H-6 causes serious problems in the use of the ^1H correlation method, and ^{13}C correlation experiments provide data crucial to a rigorous assignment. Specifically, the HMQC spectrum gives discrete cross peaks even for strongly coupled ^1H resonances due to the low natural abundance of ^{13}C and the large values of $^1J_{CH}$ which are sufficient to relieve the strong coupling. The ^{13}C chemical shift dispersion of the furanoside carbon atoms is excellent with ^{13}C resonances in characteristic positions, making possible tentative assignments on the basis of chemical shift analogies. The correctness of these assignments can then be verified by the data of the HMBC experiment. Since no proton is more than three bonds away from any ^{13}C in the ring, interpretation of HMBC data in furanosides is complicated, and the assignments of the C-6 methylene resonance by DEPT and of H-6 and H-5 by TQF-COSY were especially valuable in this case. The spin system of C-5, C-6, H-5, and H-6 for the furanoside was discretely identified by TQF, DEPT, HMQC, and HMBC, and this system was connected with the rest of the furanoside ring by HMBC correlation of C-5 with H-3.

A special problem in linkage assignment is posed by these polymers in which the oligosaccharide repeating subunits are joined by phosphodiester bonds. Although the assignment of the position of phosphodiester linkages can be difficult by classical chemical methods, rigorous identification of the phosphate positions by NMR methods was straightforward. Resolution-enhanced ^{13}C spectra revealed scalar coupling to the anomeric ^{13}C and three-bond coupling to C-2 as well as to the aglycon carbon (C-6) and to the adjacent C-5. Three-bond coupling of ^{31}P to the anomeric and aglycon proton as well as four-bond coupling to H-2 of GalNAc (residue F) in the J22 polymer was observed in the ^1H–^{31}P correlation spectra.

ACKNOWLEDGMENTS

We thank the National Magnetic Resonance Facility at Madison, supported by NIH Grant RR-02301, for providing 500-MHz NMR facilities as well as helpful advice on the experimental techniques. We acknowledge the help of Liqiang Xu for the carbohydrate analyses.

Registry No. Polysaccharide from *S. sanguis* J22, 123992-44-9.

REFERENCES

Abeygunawardana, C., Bush, C. A., Tjoa, S. S., Fennessey, P. V., & McNeil, M. R. (1989) *Carbohydr. Res. 191*, 279–293.

Altona, A., & Hasnoot, C. A. G. (1980) *Org. Magn. Reson. 13*, 417–429.

Bax, A., & Davis, D. G. (1985) *J. Magn. Reson. 65*, 355–360.

Bax, A., & Summers, M. F. (1986) *J. Am. Chem. Soc. 108*, 2093–2094.

Bax, A., & Marion, D. (1988) *J. Magn. Reson. 78*, 186–191.

Bax, A., Griffey, R. H., & Howkins, B. L. (1983) *J. Magn. Reson. 55*, 301–315.

Beier, C. R., Mundy, B. P., & Strobel, G. A. (1980) *Can. J. Chem. 58*, 2800–2804.

Bush, C. A. (1989) *Bull. Magn. Reson. 10*, 73–95.

Bush, C. A., Duben, A. J., & Ralapati, S. (1980) *Biochemistry 19*, 501–504.

Byrd, R. A., Summers, M. F., Zon, G., Fonts, C. S., & Marzilli, L. G. (1986) *J. Am. Chem. Soc. 108*, 504–505.

Byrd, R. A., Egan, W., Summers, M. F., & Bax, A. (1987) *Carbohydr. Res. 166*, 47–58.

Cisar, J. O. (1986) in *Microbial Lectins and Agglutinins: Properties and Biological Activity* (Mirelman, D., Ed.) pp 183–196, Wiley, New York.

Cisar, J. O., Kolenbrander, P. E., & McIntire, F. C. (1979) *Infect. Immun. 24*, 742–752.

Cyr, N., Hamer, G. K., & Perlin, A. S. (1978) *Can. J. Chem. 56*, 297.

Dabrowski, J., Houck, M., Romanowska, E., & Gamian, A. (1987) *Biochem. Biophy. Res. Commun. 146*, 1283–1285.

Doddrell, D. M., Pegg, D. T., & Bendall, M. R. (1982) *J. Magn. Reson. 48*, 323–327.

Dubois, M., Gilles, K. A., Hamilton, J. K., Rebers, P. A., & Smith, F. (1956) *Anal. Chem. 28*, 350–356.

Egan, W. (1980) in *Magnetic Resonance in Biology* (Cohen, J. S., Ed.) Vol. 1, pp 197–258, Wiley, New York.

Fu, J. M., Schroeder, S. A., Jones, C. R., Santini, R., & Gorenstein, D. G. (1988) *J. Magn. Reson. 77*, 577–582.

Hall, L. D., & Malcolm, R. B. (1972) *Can. J. Chem. 50*, 2092-2101.
Homans, S. W., Dwek, R. A., Boyd, J., Seffe, N., & Rademacher, T. W. (1987) *Proc. Natl. Acad. Sci. U.S.A. 84*, 1202-1205.
Jentoft, N. (1985) *Anal. Biochem. 148*, 424-433.
Jones, C. (1985) *Carbohydr. Res. 139*, 75-83.
Kaluarachchi, K. K. I., & Bush, C. A. (1989) *Anal. Biochem. 179*, 209-215.
Kumar, A., Wagner, G., Ernst, R. R., & Wuthrich, K. (1980) *Biochem. Biophys. Res. Commun. 96*, 1156-1163.
Kumar, A., Hosuy, R. V., & Chandrasekhar, K. (1984) *J. Magn. Reson. 60*, 1-6.
Laffite, C., Phnoc Du, M. C., Winterutz, F., Wylde, R., & Pratriel-Sosa, F. (1978) *Carbohydr. Res. 67*, 91-103.
Lemieux, R. U., & Koto, S. (1974) *Tetrahedron 30*, 1933-1944.
Lerner, L., & Bax, A. (1987) *Carbohydr. Res. 166*, 35-46.
Levitt, M. H., Freeman, R., & Frenkiel, T. (1982) *J. Magn. Reson. 47*, 328-330.
Marion, D., & Wuthrich, K. (1983) *Biochem. Biophys. Res. Commun. 117*, 967-974.
McIntire, F. C., Bush, C. A., Wu, S. S., Li, S. C., Li, Y. T., Tjoa, S. S., & Fennessey, P. V. (1987) *Carbohydr. Res. 166*, 133-143.
McIntire, F. C., Crosby, I. K., Vatter, A. E., Cisar, J. O., McNeil, M. R., Bush, C. A., Tjoa, S. S., & Fennessy, P. V. (1988) *J. Bacteriol. 170*, 2229-2235.
Michon, F., Brisson, J. R., Dell, A., Kasper, D. L., & Jennings, H. J. (1988) *Biochemistry 27*, 5341-5351.
Morat, C., Taravel, F. R., & Vignon, M. R. (1988) *Magn. Reson. Chem. 26*, 264-270.
Moreau, M., Richards, J. C., Perry, M. B., & Kinskern, P. J. (1988) *Biochemistry 27*, 6820-6829.
Muller, N., Ernst, R. R., & Wuthrich, K. (1986) *J. Am. Chem. Soc. 108*, 6842-6492.
Neuhaus, D., Wagner, G., Vasak, M., Kagi, J. H. R., & Wuthrich, K. (1984) *Eur. J. Biochem. 143*, 659.
Ogawa, T., & Seta, A. (1982) *Carbohydr. Res. 110*, C1-C4.
Piantini, U., Sorensen, O. W., & Ernst, R. R. (1982) *J. Am. Chem. Soc. 104*, 6800-6801.
Rance, M., Sorensen, O. W., Bodenhausen, G., Wagner, G., Ernst, R. R., & Wuthrich, K. (1983) *Biochem. Biophys. Res. Commun. 117*, 479-485.
Rao, B. N. N., & Bush, C. A. (1988) *Carbohydr. Res. 180*, 111-128.
Redfield, A. G. (1978) *Methods Enzymol. 49*, 253-270.
Richards, J. C., Perry, M. B., & Carlo, D. J. (1983) *Can. J. Biochem. Cell Biol. 61*, 178-190.
Shaka, A. J., Keelar, J., Frenkiel, T., & Freeman, R. (1983) *J. Magn. Reson. 52*, 335-338.
Shaskov, A. S., Lipkind, G. M., Knivel, V. A., & Kochetkov, N. K. (1988) *Magn. Reson. Chem. 26*, 735-747.
States, D. J., Hakerborn, R. A., & Ruben, D. J. (1982) *J. Magn. Reson. 48*, 286-292.
Widmer, H., & Wuthrich, K. (1987) *J. Magn. Reson. 74*, 316-336.
Williamson, D., & Bax, A. (1988) *J. Magn. Reson. 76*, 174-177.

Interaction of Antibodies with Fc Receptors in Substrate-Supported Planar Membranes Measured by Total Internal Reflection Fluorescence Microscopy†

Claudia L. Poglitsch and Nancy L. Thompson*
Department of Chemistry, The University of North Carolina at Chapel Hill, Chapel Hill, North Carolina 27599-3290
Received April 28, 1989; Revised Manuscript Received August 11, 1989

ABSTRACT: A procedure for constructing substrate-supported planar membranes using membrane fragments isolated from the macrophage-related cell line J774A.1 is described. Total internal reflection (TIR) fluorescence microscopy is employed to demonstrate that fluorescently labeled Fab fragments of a monoclonal antibody (2.4G2) with specificity for a murine macrophage cell-surface receptor for IgG (moFc$_\gamma$RII) bind to the planar model membranes. These measurements show that the planar membranes contain moFc$_\gamma$RII and yield a value for the association constant of 2.4G2 Fab fragments with moFc$_\gamma$RII equal to $(9.6 \pm 0.4) \times 10^8$ M^{-1} and indicate that the surface density of reconstituted moFc$_\gamma$RII is $\sim$50 molecules/μm^2. In addition, TIR fluorescence microscopy is used to investigate the Fc-mediated competition of unlabeled, polyclonal murine IgG with labeled 2.4G2 Fab fragments for moFc$_\gamma$RII in the planar membranes. These measurements indicate that the reconstituted moFc$_\gamma$RII recognized by 2.4G2 Fab fragments also retains the ability to bind murine IgG Fc regions and yield a value for the association constant of polyclonal murine IgG with moFc$_\gamma$RII equal to $(1-5) \times 10^5$ M^{-1}. This work represents one of the first applications of TIR fluorescence microscopy to specific ligand-receptor interactions.

One mechanism of immunological defense is phagocytosis, in which macrophage cells ingest and destroy pathogenic organisms (Riches et al., 1988). In receptor-mediated phagocytosis, Fc receptors on a macrophage cell surface recognize IgG-coated targets and signal the macrophage to ingest the target (Unkeless et al., 1988). Murine macrophages have at least three distinct cell-surface IgG Fc receptors, and at least one of these receptors (moFc$_\gamma$RII) has been implicated in the phagocytotic process (Unkeless et al., 1981, 1988). Biochemical and immunological characterization of moFc$_\gamma$RII has been facilitated by the development of a rat-mouse hy-

†This work was supported by National Institutes of Health Grant GM-37145, by National Science Foundation Presidential Young Investigator Award DCB-8552986, and by E. I. du Pont de Nemours and Co.
*To whom correspondence should be addressed.

0006-2960/90/0429-248$02.50/0